

**LABORATORY STUDY OF HEALING
EFFECTIVENESS OF SALT FRACTURES
UNDER NORMAL STRESSES
AND TEMPERATURES**

Prueangprach Charoenpiew



**A Thesis Submitted in Partial Fulfillment of the Requirements for the
Degree of Master of Engineering in Geotechnology
Suranaree University of Technology
Academic Year 2015**

การศึกษาการเชื่อมประสานของรอยแตกในเกลือหินภายใต้ความกดดันตั้งฉาก
และอุณหภูมิ



วิทยานิพนธ์นี้เป็นส่วนหนึ่งของการศึกษาตามหลักสูตรปริญญาวิศวกรรมศาสตรมหาบัณชิต
สาขาวิชาเทคโนโลยีธรณี
มหาวิทยาลัยเทคโนโลยีสุรนารี
ปีการศึกษา 2558

**LABORATORY STUDY OF HEALING EFFECTIVENESS OF
SALT FRACTURES UNDER NORMAL STRESSES AND
TEMPERATURES**

Suranaree University of Technology has approved this thesis submitted in partial fulfillment of the requirements for a Master's Degree.

Thesis Examining Committee

(Dr. Prachya Tepnarong)

Member (Thesis Advisor)

(Prof. Dr. Kittitep Fuenkajorn)

Member

(Asst. Prof. Dr. Decho Phueakphum)

Chairperson

(Prof. Dr. Sukit Limpijumnong)

Vice Rector for Academic Affairs
and Innovation

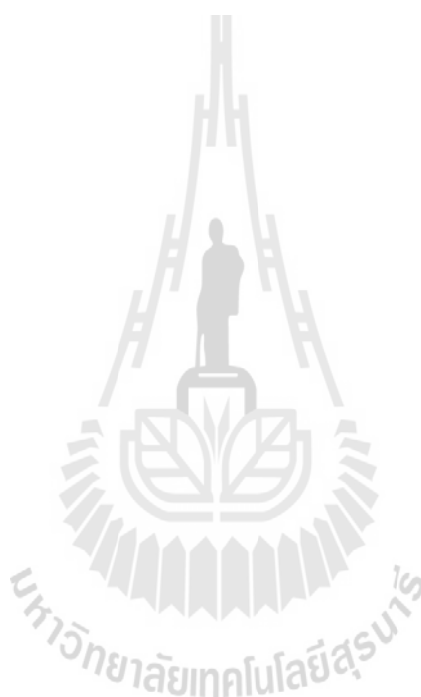
(Assoc. Prof. Ft. Lt. Dr. Kontorn Chamniprasart)

Dean of Institute of Engineering

เป็รื่องปรัชญ์ เจริญพิว : การศึกษาการเชื่อมประสานของรอยแตกในเกลือหินภายใต้ความ
เค้นต้งฉากและอุณหภูมิ (LABORATORY STUDY OF HEALING EFFECTIVENESS
OF SALT FRACTURES UNDER NORMAL STRESSES AND TEMPERATURES)
อาจารย์ที่ปรึกษา : อาจารย์ ดร.ปรัชญ์ เทพณรงค์, 67 หน้า.

วัตถุประสงค์ของงานวิจัยเพื่อศึกษาความสามารถในการเชื่อมประสานของรอยแตกของ
เกลือหินที่ได้รับผลกระทบจากสภาวะความเค้น ชนิดของรอยแตก เวลา และ อุณหภูมิ ในการศึกษา
นี้ได้ทดสอบการเชื่อมประสานของรอยแตกภายใต้ความเค้นกดตั้งฉากจาก 0.5, 1.0, 1.5 และ 2.0
MPa เป็นระยะเวลา 56 วัน และภายใต้ความเค้นกดที่เท่ากันทุกทิศทางที่ระดับ 5 และ 10 MPa เป็น
ระยะเวลา 0, 6, 12, 24, 72, 120 และ 168 ชั่วโมง อุณหภูมิที่ใช้ในการทดสอบสำหรับการเชื่อม
ประสานภายใต้ความเค้นตั้งฉากคือ 25, 70, 150 และ 200°C และอุณหภูมิที่ใช้ในการทดสอบการ
เชื่อมประสานภายใต้ความเค้นกดที่เท่ากันทุกทิศทางคือที่อุณหภูมิห้อง และ 200°C คลื่นอัลตรา
โซนิคทั้งคลื่นปฐมภูมิ (P-wave) และคลื่นทุติยภูมิ (S-wave) ได้ถูกตรวจวัดกับตัวอย่างรอยแตกที่
ทดสอบภายใต้ความเค้นกดตั้งฉากเค้นตั้งฉากทุก 7 วัน ตลอดระยะเวลา 56 วัน ตัวอย่างรอยแตก
ภายหลังจากที่มีการเชื่อมประสานภายใต้ความเค้นกดตั้งฉากได้ถูกทดสอบกำลังรับแรงกดแบบจุด
กด และทดสอบกำลังรับแรงกดแบบเส้นบนตัวอย่างรอยแตกหลังจากการเชื่อมประสานภายใต้
ความเค้นกดที่เท่ากันทุกทิศทางเพื่อทำการประเมินประสิทธิภาพการเชื่อมประสานของรอยแตกใน
เกลือหิน ผลการศึกษาพบว่ารอยแตกจากการแยกของผลึกหรือรอยแตกจากการตัดด้วยเลื่อย
(Series I) บ่งชี้ว่ารอยแตกยังคงแยกออกจากกันโดยไม่มีเการเชื่อมประสานแต่อย่างใด โดยเฉพาะ
อย่างยิ่งถ้ามีรอยแตกเต็มไปด้วสิ่งเจือปนต่างๆ ก็จะไม่เกิดการเชื่อมประสานขึ้น สำหรับรอยแตก
แบบการทำให้แยกออกโดยแรงดึง (Series II and III) บ่งชี้ว่าความสามารถในการเชื่อมประสานจะ
เพิ่มขึ้นเมื่อความเค้นและเวลาเพิ่มขึ้น ซึ่งสอดคล้องกับผลการทดลองในเกลือหินที่ดำเนินการโดย
(Fuenkajorn and Phueakphum, 2011) การเชื่อมประสานของรอยแตกภายใต้ความเค้นอัดที่เท่ากัน
ทุกทิศทางมีความได้เปรียบกว่าการเชื่อมประสานภายใต้ความเค้นตั้งฉากเนื่องจากสามารถทดสอบ
ภายใต้ความเค้นที่ระดับสูงกว่าได้ ในขณะที่การทดสอบการประสานภายใต้ความเค้นกดตั้งฉาก
เพียงอย่างเดียวนั้นการให้ความเค้นกดสูงสุดจะถูกจำกัดด้วค่ากำลังรับแรงกดสูงสุดของเกลือหิน
ในการทดสอบนี้ความเค้นกดตั้งฉากสูงสุดที่ใช้มีค่าเท่ากับ 2 MPa หรือประมาณ 5% ของกำลังกด
สูงสุดในแกนเดียวของเกลือหิน โดยการทดสอบภายใต้ความเค้นกดล้อมรอบที่เท่ากันทุกทิศทาง
ตัวอย่างสามารถกระทำด้วภายใต้ความเค้นสูงถึง 10 MPa ด้วยเหตุนี้จึงทำให้การเชื่อมประสาน
ภายใต้ความเค้นกดล้อมรอบที่เท่ากันทุกทิศทางมีประสิทธิภาพสูงกว่าการเชื่อมประสานภายใต้

ความเค้นกดตั้งฉากเพียงอย่างเดียว ส่วนความเร็วคลื่นที่ทำการตรวจวัดบนตัวอย่างเกลือหินมีแนวโน้มเพิ่มขึ้นอย่างรวดเร็วในช่วง 7 วันแรกของการทดสอบและหลังจากนั้นคลื่นปฐมภูมิมีการเพิ่มขึ้นเพียงเล็กน้อยเท่านั้นเมื่อเวลาเพิ่มขึ้น สำหรับการเชื่อมประสานภายใต้ความเค้นกดที่เท่ากันทุกทิศทาง ผลการศึกษาระบุว่าความสามารถในการเชื่อมประสานมีแนวโน้มเพิ่มขึ้นเมื่อระยะเวลาในการเชื่อมประสานและความเค้นอัดล้อมรอบที่เท่ากันมีการเพิ่มขึ้น อุณหภูมิทำให้ความสามารถในการเชื่อมประสานเพิ่มขึ้นเพียงเล็กน้อย



สาขาวิชา เทคโนโลยีธรณี
ปีการศึกษา 2558

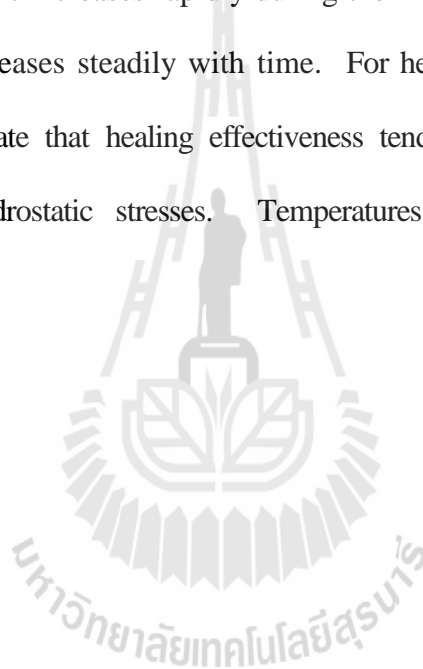
ลายมือชื่อนักศึกษา _____
ลายมือชื่ออาจารย์ที่ปรึกษา _____

PRUEANGPRACH CHAROENPIEW : LABORATORY STUDY OF HEALING
EFFECTIVENESS OF SALT FRACTURES UNDER NORMAL STRESSES
AND TEMPERATURES. THESIS ADVISOR : PRACHYA TEPNARONG,
Ph.D., 67 PP

HEALING/ ROCK SALT/ FRACTURE/TEMPERATURE/TIME/STRESS

The objective of this study is to assess the healing effectiveness of rock salt fractures as affected by the stress conditions, fracture types, time and temperatures. The effort involved healing tests under constant axial stresses from 0.5, 1.0, 1.5 and 2.0 MPa within 56 days and hydrostatic stresses from 5 and 10 MPa within 0, 6, 12, 24, 72, 120 and 168 hour. The temperatures are varied from 25, 70, 150 and 200°C for healing under uniaxial stresses and temperatures are ambient and 200°C for healing under hydrostatic stresses tests. The ultra-sonic wave, P-wave and S-wave, are monitored on healed fractures under axial stresses for every 7 days throughout 56 days. The point load tests on the healed fractures under axial stresses and line load tests on healed fracture under hydrostatic stresses are performed to assess the mechanical performance of the fractures after healing. The results indicated that the fractures formed by separation of inter-crystalline boundaries or saw-cut fractures (Series I) remained separable with no healing. In particular, if the fracture surface is coated with any inclusions, healing will not occur. For tension-induced fracture (Series II and III), the healing effectiveness increase with increasing stresses and time these agree with the experimental results on rock salt performed by (Fuenkajorn and Phueakphum, 2011). Fracture healing under hydrostatic stresses has an advantage over that healing under

axial stresses, in term of the maximum applied stresses. The applied stress is limited by the compressive strength of rock salt. The maximum axial stress used here is therefore limited to 2 MPa or about 5% of the strength. This is primarily to prevent the initiation of fractures in the intact salt. For the hydrostatic stresses, the specimen can subject to hydrostatic as high as 10 MPa. Fracture healing under hydrostatic stresses has more efficiency than those healing under axial stresses. The wave velocity of the rock salt increases rapidly during the first 7 days, and after that the P-wave are slightly increases steadily with time. For healing under hydrostatic stresses tests, the results indicate that healing effectiveness tended to increase with increasing healing time and hydrostatic stresses. Temperatures slightly increase the healing effectiveness.



School of Geotechnology

Academic Year 2015

Student's Signature _____

Advisor's Signature _____

ACKNOWLEDGMENTS

I wish to acknowledge the funding supported by Suranaree University of Technology (SUT).

I would like to express my sincere thanks to Dr. Prachya Tepnarong for his valuable guidance and efficient supervision. I appreciate his strong support, encouragement, suggestions and comments during the research period. My heartiness thanks to Prof. Dr. Kittitep Fuenkajorn and Asst. Prof. Dr. Decho Phueakphum for their constructive advice, valuable suggestions and comments on my research works as thesis committee members. Grateful thanks are given to all staffs of Geomechanics Research Unit, Institute of Engineering who supported my work.

Finally, I would like to thank beloved parents for their love, support and encouragement.

Prueangprach Charoenpiew

TABLE OF CONTENTS

	Page
ABSTRACT (THAI)	I
ABSTRACT (ENGLISH).....	III
ACKNOWLEDGEMENTS	V
TABLE OF CONTENTS.....	VI
LIST OF TABLES	IX
LIST OF FIGURES	XI
SYMBOLS AND ABBREVIATIONS.....	XV
CHAPTER	
I INTRODUCTION	1
1.1 Background and rationale	1
1.2 Research objectives.....	4
1.3 Research methodology.....	5
1.3.1 Literature review.....	6
1.3.2 Sample preparation	6
1.3.3 Laboratory testing.....	7
1.3.4 Calibration of healing effectiveness, time, stresses and temperature parameters.....	7
1.3.5 Development of healing effectiveness criteria	8
1.3.6 Discussions, conclusions and thesis writing.....	8

TABLE OF CONTENTS (Continued)

	Page
1.4 Scope and limitations	8
1.5 Thesis contents	9
II LITERATURE REVIEW	10
2.1 Introduction	10
2.2 Healing fractures in rock salt	10
2.3 The effect of temperatures, time and stresses on healing fractures	15
III SAMPLE PREPARATION	19
3.1 Sample preparation	19
IV LABORATORY TESTING	26
4.1 Introduction	26
4.2 Test methods	26
4.2.1 Healing under uniaxial stresses	27
4.2.2 Healing under hydrostatic stresses	29
4.3 Test results	34
4.3.1 Healing under uniaxial stresses results	34
4.3.2 Wave velocity test results	37
4.3.3 Healing under hydrostatic stresses results	42
4.4 Discussion and conclusions	42

TABLE OF CONTENTS (Continued)

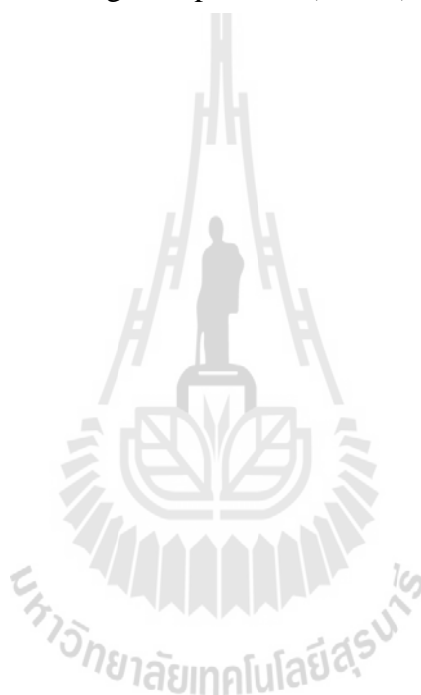
	Page
V DEVELOPMENT OF HEALING EFFECTIVENESS CRITERIA	46
5.1 Objectives	46
5.2 Healing effectiveness criterion	46
5.2.1 Healing under uniaxial stresses criterion	46
5.2.2 Healing under hydrostatic stresses criterion	48
5.3 Applications	52
5.4 Discussion of the results	56
VI DISCUSSIONS, CONCLUSIONS AND	
RECOMMENDATIONS FOR FUTURE STUDIES	58
6.1 Discussions	58
6.2 Conclusions	60
6.3 Recommendations for future studies	63
REFERENCES	64
BIOGRAPHY	67

LIST OF TABLES

Table	Page
3.1 Cylindrical salt specimens prepared for healing test by subjecting uniaxial loading under ambient temperature.....	24
3.2 Cylindrical salt specimens prepared for healing test by subjecting uniaxial loading under elevated temperature at 70, 150 and 200°C.....	25
3.3 Rectangular salt specimens prepared for healing test by subjecting confining pressure under ambient temperature and under elevated temperature of 200°C.....	25
4.1 Summarized the parameters for healing test of salt fracture.....	28
4.2 Point load strength index test results obtained for the healed tension-induced fracture which tested under uniaxial stresses at ambient room temperature.....	36
4.3 Point load strength index test results obtained for the healed tension-induced fracture which tested under uniaxial stresses at elevated temperature.....	37
4.4 Wave velocity test results for elastic modulus after healing under constant axial stress, elevated temperatures and healing time.....	40
4.5 Healing test under hydrostatic stresses. The fracture healing effectiveness is assessed by elevated temperatures and time.....	44
5.1 Empirical constants obtained for the healing of salt fracture under uniaxial stresses conditions at ambient temperature (25°C).....	47

LIST OF TABLES (Continued)

- 5.2 Empirical constants obtained for the healing of salt fracture under hydrostatic stresses conditions at ambient temperature (25°C)50
- 5.3 Empirical constants obtained for the healing of salt fracture under hydrostatic stresses conditions at high temperature (200°C)51



LIST OF FIGURES

Figure	Page
1.1 Research methodology.....	5
2.1 Healing test under uniaxial loading. The specimens are loaded axially by means of a dead weight consolidation machine (Fuenkajorn and Phueakphum, 2011)...	11
2.2 Specimens with tension-induced fracture (a) and with polished fracture (b) (Fuenkajorn and Phueakphum, 2011).....	12
2.3 Hydraulic conductivity (K_f) of five tension-induced fractures as a function of time (t) under static loading (Fuenkajorn and Phueakphum, 2011).....	12
2.4 Value of lateral initial stress damage vs. value of damage in stable stage Jiang et al. (2013).....	16
2.5 Damage variation and time relation curve .The relationship between wave velocity and time curve of rock salts at room temperature, 50 °C and 70 °C (Chen et al., 2013).....	17
3.1 Two types of fractures: saw-cut fracture and tension-induced fracture.....	21
3.2 Saw-cut fracture specimens are dry-cut by a cutting device.....	21
3.3 Tension induces fractures specimen by point load strength index test.....	22
3.4 Some rectangular shaped salt specimen with nominal dimensions of 44×44×88 mm in prepared and then it is subjected by line load to induced tensile fracture.....	22
3.5 Some salt specimen with the tension-induce fracture by line load.....	23

LIST OF FIGURES (Continued)

Figure	Page
4.1 Test setup for healing test under the uniaxial stress at ambient temperature. The dead weights from steel plates are applied on the top of rock sample to induce the uniaxial stress on salt fractures.....	30
4.2 The heating equipment is used to heat the specimen during healing testing. The salt specimens will be wrapped with heating tape, foil and insulator before testing. The regulator (right) used to controls the temperature on rock sample.....	31
4.3 A salt specimen is wrapped with heating tape, foil and isolator before testing to maintain constant during the test.....	31
4.4 Test setup for healing test under the uniaxial stress at elevated temperatures	32
4.5 Polyaxial load frame (Fuenkajorn and Kenkhunthod, 2010) used to apply constant hydrostatic stresses on the rock sample.....	32
4.6 Heater coil entwined around steel platen before applied to the rock specimen	33
4.7 Temperatures measured and regulated are made by thermocouples and thermostats.....	33
4.8 Thermostat is a component of a control system which senses the temperature of a system so that the system's temperature is maintained near a desired set point	35
4.9 The test setup for determining the point load strength index of healed fracture.....	35

LIST OF FIGURES (Continued)

Figure	Page
4.10	Healing effectiveness as a function of healing time obtained from healing test under axial loading on the tension-induced fractures at ambient temperature.....
	39
4.11	Healing effectiveness for 56 days of healing time as a function of temperatures obtained from healing test on the tension-induced fractures under elevated temperature.....
	39
4.12	Wave velocity measurements after fracture healing under uniaxial loading.....
	40
4.13	P-wave velocities (H_e) as a function of time (t) of tension-induced fractures at uniaxial stresses 0.5 MPa. P-wave velocities (H_e) as a function of time (t) of tension-induced fractures at ambient temperature.....
	41
4.14	Healing effectiveness as a function of healing time obtained from healing test under hydrostatic stresses loading (5 and 10 MPa) at ambient temperature and at elevated temperature of 200°C.....
	45
4.15	Healing effectiveness (at 168 hours) as a function of temperatures obtained from healing test under hydrostatic stress loading of 5 and 10 MPa.....
	45
5.1	Healing under uniaxial tests as a function of healing time: test results (points), regression analysis results (solid lines) and prediction (dashed line).....
	48
5.2	Healing under hydrostatic stresses tests at ambient temperature as a function of healing time, test results (points) and back predictions (lines).....
	49

LIST OF FIGURES (Continued)

Figure	Page
5.3	Healing under hydrostatic stresses tests at high temperature as a function of healing time, test results (points) and back predictions (lines).....
	51
5.4	Stresses around salt cavern and induced fracture during minimum pressure of operation.....
	53
5.5	Healing effectiveness as a function of the variable of (r/a) ratio. This figure used the equation 5.1 for predicted healing effectiveness.....
	55
5.6	Healing effectiveness as a function of the variable of (r/a) ratio. This figure used the equation 5.2 for predicted healing effectiveness.....
	56

SYMBOLS AND ABBREVIATIONS

T	=	Absolute temperature
α	=	Empirical constant
β	=	Empirical constant
δ	=	Empirical constant
κ	=	Empirical constant
ω	=	Empirical constant
η	=	Empirical constant
λ	=	Empirical constant
ψ	=	Empirical constant
φ	=	Empirical constant
ζ	=	Empirical constant
ξ	=	Empirical constant
H_e	=	Healing effectiveness
σ_{Axial}	=	Major Principal Stress
$\sigma_{\text{Hydrostatic}}$	=	Minor principal stress
t	=	Time

CHAPTER I

INTRODUCTION

1.1 Background and rationale

The challenge on the underground excavation in salt and potash formation (such as solution mining and room and pillar mining) and the underground facilities related with salt mining such as solution cavern for storage technology (such as compressed-air energy storage, natural gas storage, nuclear waste disposal in salt mining) are that the cracks or fractures induced by naturally occurring and the damage during excavation may cause instability of the surrounding salt and leakage of storage materials from cavern. However, self-healing can impel the fracture of damaged rock salt, thereby improving the mechanical properties and permeability of damaged rock salt inside the cavern. Damage in rock salt which generally manifests in the form of micro-cracks and fractures can be recovered or healed when subjected to sufficiently under confinement (hydrostatic and non-hydrostatic) and temperatures. When cracks are closed, permeability can be reduced by several orders of magnitude (Renard, 1999). The healing capability of fractures is one of the advantages for rock salt to be used as a host rock for the nuclear waste repository, hazardous chemical, natural gas storage and compressed-air energy storage. The presence of damage in the form of micro-cracks in salt can alter the structural stability and permeability of salt, affecting the integrity of a repository (Chen et al., 1998). The healing of rock salt fractures around air or gas storage caverns also affects the designed storage

capacity and the mechanical stability of the caverns (Katz and Lady, 1976). Miao et al. (1995) state that healing of rock salt is probably due to the visco-plastic deformation of grains which causing the closure of cracks and pore spaces. The size reduction of the micro-cracks can increase the salt stiffness and strength. The main driving force for fracture healing is a minimization of surface tension, and creation of contact areas and covalent bonds between the two surfaces of the fracture.

Salt damage may induce in micro-scaled (micro-cracking) to large-scaled of discontinuities (fractures). The change of pressure and temperature during pressure release from the compressed-air cavern to produce the electricity in high energy demand period will induced and propagated of fractures in salt around the cavern. The temperature induced by the chemical reaction from waste has an effect on mechanical stability of the storage cavity. The initiation, propagation and healing of fractures in salt mass around underground structures have long been recognized; most investigations however have concentrated on their impact on the mechanical constitutive behavior of the rock (e.g., Allemandou and Dusseault 1993; Munson et al. 1999). Several experimental researches on the healing and consolidation of crushed salt have also been carried out in an attempt at understanding the healing behavior between the salt particles and their impact on the bulk properties (e.g., Ouyang and Daemon, 1989; Miao et al., 1995). Chen et al. (2013) uses ultrasonic technology to monitor the longitudinal wave velocity variations during self-healing under constant stress and several of temperatures. Micro-cracks can be healed by recrystallization, but the process is difficult. More stress-induced initial damage results in more internal macro-cracks, leading to a more difficult recovery. Temperature baking only does not favor self-healing because higher temperature

results in a more difficult recovery. Under constant recovery temperature with constant humidity, the rise of temperature promotes grain recrystallization that is beneficial to damage recovery. However, they research was not performed the mechanical test to assess the healing effectiveness of healed fractures. Fuenkajorn and Phueakphum (2011) performed the laboratory to assess the healing effectiveness of rock salt fractures as affected by the stress conditions, fracture types, and time. The effort involved healing tests under uniaxial and radial pressures, gas flow permeability tests to monitor the time-dependent behavior of the salt fractures, and point loading and diameter loading tests to assess the mechanical performance of the fractures after healing. Healing tests under static loading are were carried out under both dry and saturated conditions. The results suggest that the primary factors governing the healing of salt fractures are the origin and purity of the fractures, and the magnitude and duration of the fracture pressurization. Inclusions or impurities significantly reduce the healing effectiveness. The hydraulic conductivity of the fractures in pure salt can be reduced permanently by more than 4 orders of magnitude under the applied stress of 20 MPa for a relatively short period. For most cases the reduction of salt fracture permeability is due to the fracture closure which does not always lead to fracture healing. The closure involves visco-plastic deformation of the asperities on both sides of the salt fracture, while the healing is related to the covalent bonding between the two surfaces. Fracture roughness and brine saturation apparently have an insignificant impact on the healing process. However, they performed only with the short period and not considered the influencing of temperature during the fractured healing for representing the real condition that are under high temperature such as nuclear waste repository storage.

For nuclear waste repository, the mechanical stability and hydraulic performance need to provide for the long period up to 200,000 years (Damjanac, 2008). It is necessary to study the healing of rock salt fracture under high temperature and long-term duration on different types of salt fractures (saw-cut surface and tension induced surface). It can be reveal how to prevent the leakage of the nuclear waste or chemicals which may affect the environment in and surrounding areas by the mechanisms of fracture healing under such conditions.

1.2 Research objectives

The objective of this study is to assess the healing effectiveness of rock salt fractures as affected by the stress conditions, fracture types and time. The effort involved healing tests under constant axial loading (various from 0.5, 1.0, 1.5 and 2.0 MPa) and radial loadings (various from 2, 5, 10 and 15 MPa) within 56 days. The temperatures are varied from 25, 70, 150 and 200°C. Gas flow permeability test are performed every 7 days throughout 56 days to assess the healing effectiveness under radial loading. The ultra-sonic wave, P-wave and S-wave, are monitored on healed fractures under axial loading in every 7 days throughout 56 days. The mechanical testing; the point load tests on healed fracture under axial loading and line load tests on healed fracture under radial loading are performed to assess the mechanical performance of the fractures after healing. The results are compared the mechanical properties of healed fracture with intact salt to determine the healing effectiveness under the test conditions and developed the mathematical relationships between the healing effectiveness as a function of stresses, time and temperatures.

1.3 Research methodology

The research methodology shown in Figure 1 comprises 7 steps; including literature review, sample preparation, laboratory testing, computer simulation, discussions and conclusions and thesis writing.

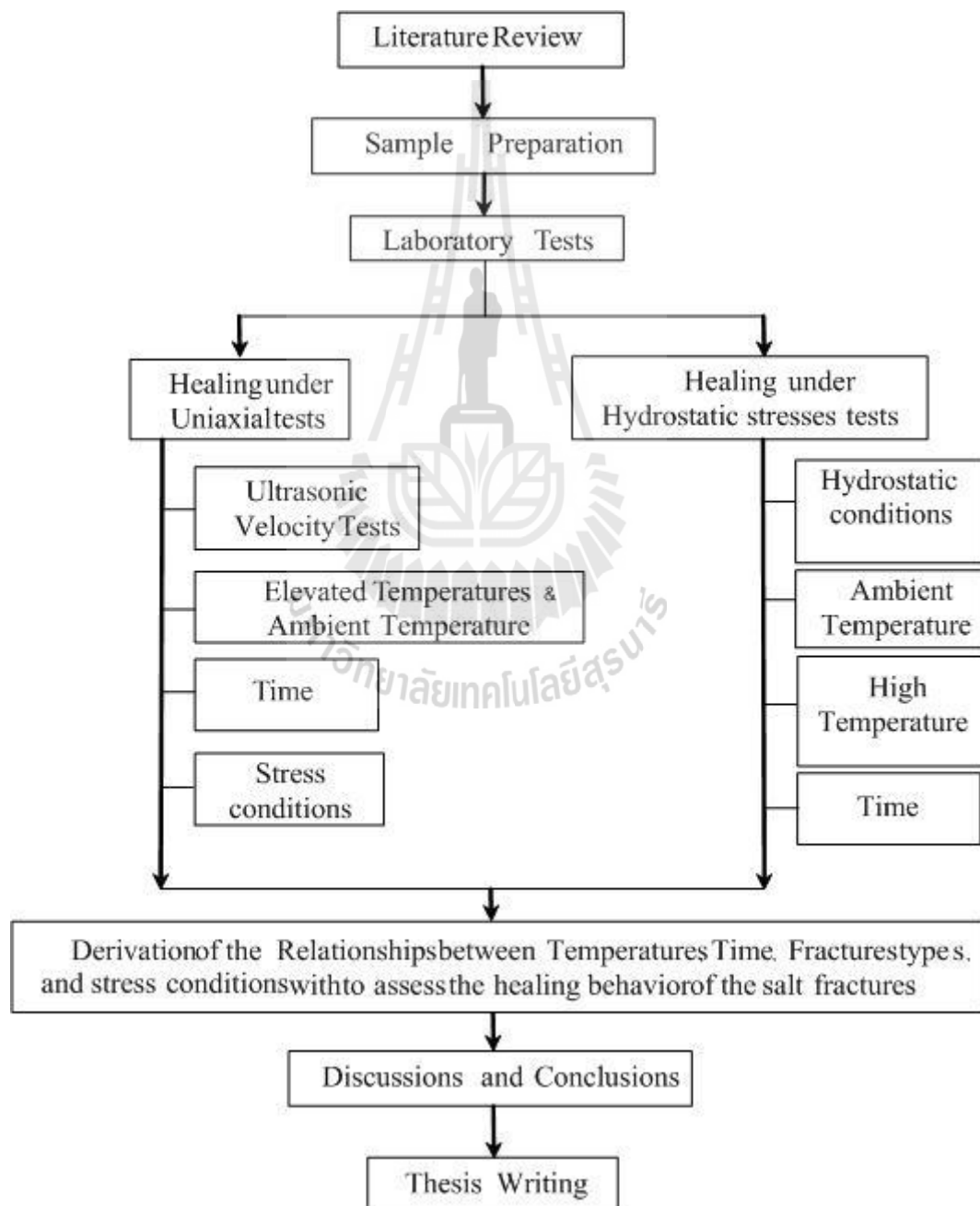


Figure 1 Research methodology.

1.3.1 Literature review

Literature reviews are carried out to study the previous researches on the mechanical and hydraulic properties of healed fractures under confinement, temperature and time. The mechanism of fracture healing and the method to measure the healing effectiveness by using various techniques such as the changing of ultrasonic wave, changing of fracture hydraulic conductivity, and the increasing of mechanical properties. The sources of information are from text books, journals, technical reports and conference papers. A summary of the literature review are given in the thesis.

1.3.2 Sample preparation

The salt specimens used were drilled from the Middle or Lower members of the Maha Sarakham Formation in the Khorat Basin, northeast of Thailand. The core specimens were from depths ranging between 250 and 400 m. The drilling was carried out by the Siam Submanee Co., Ltd. The compressive and tensile strengths of the salt are determined. These properties are need for determining the healing test parameters. The nominal diameter of all specimens was 48 mm. The sample preparation and test procedures followed as much as practical the ASTM standard practices (i.e. ASTM D2938, ASTM D3967, ASTM D4543 and ASTM D5731). To obtain the tension-induced fractures, the cylindrical specimens are subjected to point loading or diameter loading (Brazilian tension test). The point-loaded fractures are normal to the specimen axis, and are prepared for healing under uniaxial loading. The diameter-loaded fractures are parallel to the specimen axis, and are healed under radial loading. The fracture formed by saw-cut surfaces is also normal to the specimen axis. Prior to pressurization the types and amounts of

inclusions on the fracture surfaces are determined and mapped by visual observation. The aerial percentages of the inclusions are calculated with respect to the total fracture area. These inclusions included all associated and foreign minerals or materials that are not sodium chloride.

1.3.3 Laboratory testing

Two types of salt fractures are simulated in the laboratory: 1) tension-induced fractures and 2) fractures formed by saw-cut surfaces. All fractures are well mated. Two loading schemes are employed to assess the healing behavior of the salt fractures: uniaxial (normal) loading, and radial loading. The loading are maintained constant at 0.5, 1.0, 1.5 and 2.0 MPa for the axial loading and at 5 and 10 MPa for the healing under confining pressure test. To study the influencing of temperature on fractures healing, the temperatures are varies from 25, 70, 150 and 200°C for healing under uniaxial test and constant temperatures for healing under confining pressure tests are ambient and 200°C. The ultra-sonic wave, P-wave and S-wave, are monitored on healed fractures under axial loading in every 7 days throughout 56 days. The mechanical testing; the point load tests on healed fracture under axial loading and The splitting tensile strength (Line load) tests on healed fracture under confining pressure test are performed to assess the mechanical performance of the fractures after healing.

1.3.4 Calibration of healing effectiveness, time, stresses and temperature parameters

The results are used to determine the healing effectiveness, time, stresses and temperature parameters. The regression analysis on the tests data using

SPSS statistical software (Wendai, 2000) is performed to determine the healing effectiveness, time, stresses and temperature parameters.

1.3.5 Development of healing effectiveness criteria

Results from laboratory measurements in terms of stresses, time and temperatures of rock salt are used to develop healing effectiveness criteria relationship between stresses, time and temperature. Various formulations of healing effectiveness dependent stresses, time and temperature are derived.

1.3.6 Discussions, conclusions and thesis writing

Discussions are made to determine the influence of temperature, time and loading conditions on fractures healing for analyzing the underground engineering structure stability on rock salt formations. All research activities, methods and results are documented and compiled in the thesis. The research or findings are published in the conference proceedings or journals.

1.4 Scope and limitations

The scope and limitations of the research include as follows.

- 1) All testing are conducted on the rock salt specimens obtained from the Maha Sarakham formation.
- 2) Two types of fractures are prepared for testing; tension-induced fractures and smooth fractures formed by saw-cut. All fractures should be well mated.
- 3) The test procedures will follow the relevant ASTM standard practices, as much as practical
- 4) All testing are performed under dry condition.

- 5) All samples are used to test up to 56 days.
- 6) Two series of loading conditions; the axial and radial loadings. The applied normal stress are maintained constant at 0.5, 1.0, 1.5 and 2.0 MPa and confining stress at 2, 5, 10 and 15 MPa.
- 7) The temperatures are varied from 25, 70, 150 and 200°C.
- 8) Gas flow permeability test are performed every 7 days throughout 56 days to assess the healing effectiveness under radial loading.
- 9) The ultra-sonic wave, P-wave and S-wave, are monitored on healed fractures under axial loading in every 7 days throughout 56 days.
- 10) The mechanical testing; the point load tests on healed fracture under axial loading and diameter loading (Brazilian tension test) on healed fracture under radial loading are performed to assess the mechanical performance of the fractures after healing.

1.5 Thesis contents

Chapter I describes the objectives, the problems and rationale, and the methodology of the research. Chapter II present results of the literature review on healing effectiveness of salt fractures under normal stresses and temperatures, and constitutive models with incorporating temperature effects, stresses, and time. Chapter III describes the salt sample collection and preparation. Chapter IV describes the laboratory testing and test results. Chapter V describes the healing effectiveness as affected by stresses, temperatures and time. Chapter VI summarizes the research results, and provides recommendations for future research studies.

CHAPTER II

LITERATURE REVIEW

2.1 Introduction

Literature review will be carried out to study the previous researches on the mechanical and hydraulic properties of healed fractures under confinement, temperature and time. The mechanism of fracture healing and the method to measure the healing effectiveness by using various techniques such as the changing of ultrasonic wave, changing of fracture hydraulic conductivity, and the increasing of mechanical properties. The sources of information are from text books, journals, technical reports and conference papers. The initial literature reviews are summarized as follows.

2.2 Healing fractures in rock salt

Fuenkajorn and Phueakphum (2011) performed the laboratory to assess the healing effectiveness of rock salt fractures as affected by the stress conditions, fracture types, and time. The effort involved healing tests under uniaxial and radial loading (Figure 2.1 and Figure 2.2), gas flow permeability tests to monitor the time-dependent behavior of the salt fractures, and point loading and diameter loading tests to assess the mechanical performance of the fractures after healing. Healing tests under static loading are were carried out under both dry and saturated conditions. The results suggest that the primary factors governing the healing of salt fractures are the origin and purity of the fractures, and the magnitude and duration of the fracture pressurization.

Inclusions or impurities significantly reduce the healing effectiveness. The hydraulic conductivity of the fractures in pure salt can be reduced permanently by more than 4 orders of magnitude under the applied stress of 20 MPa for a relatively short period (Figure 2.3). For most cases the reduction of salt fracture permeability is due to the fracture closure which does not always lead to fracture healing. The closure involves visco-plastic deformation of the asperities on both sides of the salt fracture, while the healing is related to the covalent bonding between the two surfaces. Fracture roughness and brine saturation apparently have an insignificant impact on the healing process.

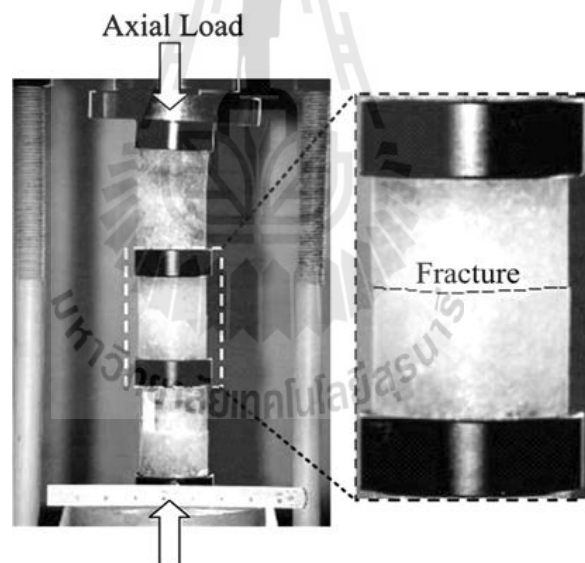


Figure 2.1 Healing test under uniaxial loading. The specimens are loaded axially by means of a dead weight consolidation machine (Fuenkajorn and Phueakphum, 2011).

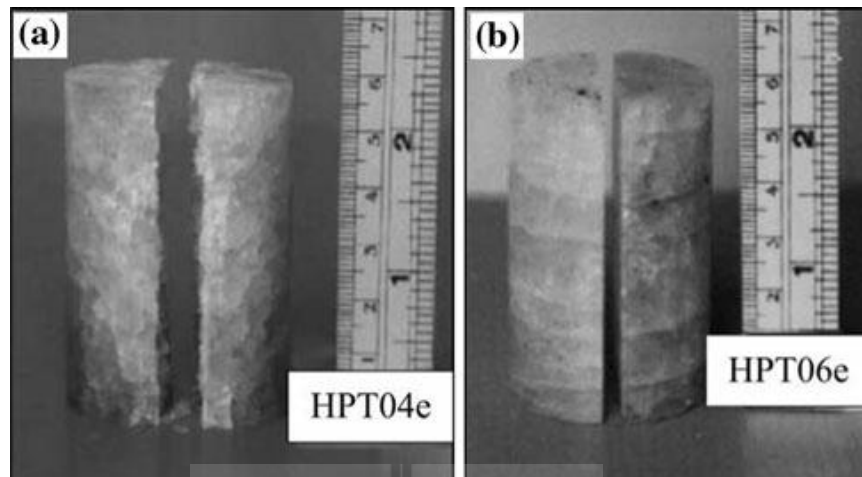


Figure 2.2 Specimens with tension-induced fracture (a) and with polished fracture (b) (Fuenkajorn and Phueakphum, 2011).

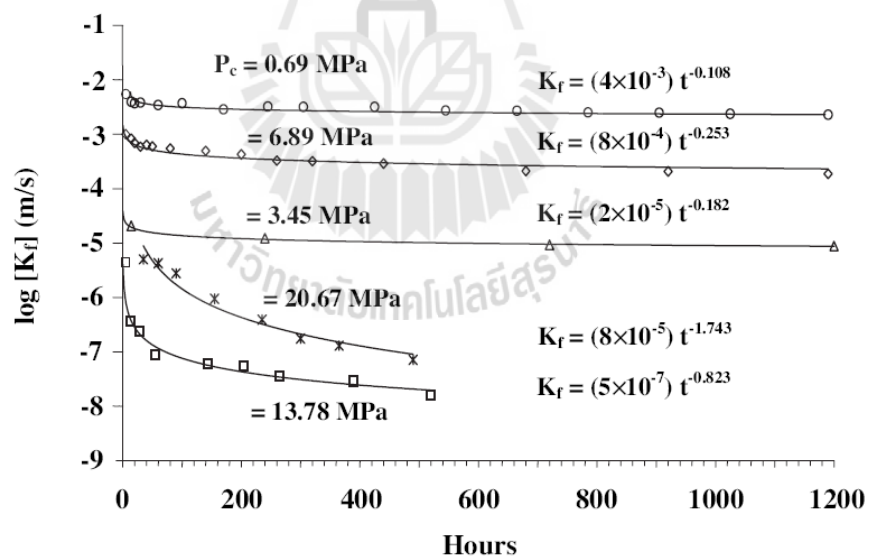


Figure 2.3 Hydraulic conductivity (K_f) of five tension-induced fractures as a function of time (t) under static loading (Fuenkajorn and Phueakphum, 2011).

Healing is closure of fracture or faults without any precipitation of matters inside the fracture. It is a chemical and physical process in which the material properties evolve with time or in which defects including voids and cracks decrease. Healing of rock salt due to visco-plastic deformation of grain, causing the closure of crack and pore space. There are two healing mechanisms, closure of micro-cracks and healing of micro-crack. It implies that micro-cracks and micro-voids reduce in size, with a corresponding increase in stiffness and strength (Miao et al., 1995). The main driving force for crack healing is a minimization of surface tension. Healing occurs by creation of contact areas and covalent bonds between the two surfaces of the fracture. It involves a local transport of mineral material. The most important factors that may affect the rate of crack healing are time, stress, temperature, saturation, contact area and geometry of contact surface, and chemical effects that may alter diffusion coefficient (Renard, 1999). In most cases, crack healing is achieved at grain size scale (micrometer to millimeter). The only way to observe healed crack may be through some tiny fluid inclusions which can be related to deformation phases or metamorphic conditions. Damage in rock salt can be healed under hydrostatic compression and also occurred under non-hydrostatic compression (Chan, et al., 1995a; 1998b; 2000).

Healing of rock fractures has occurred on various scales. In geology, fracture healing is an important mechanism controlling the circulation of fluid in the earth crust (Renard, 1999). In a smaller scale, circulation of solution or fluid in rock mass can result in a precipitation or deposition of minerals and ores in fracture zone. When fractures are open, fluid can percolate and react with in the rock (dissolution, precipitation of minerals, ore, etc.). This process notably modifies the fluid circulation and interactions between the lower crust and the surface. Healing reduces the fluid flow

between fault zones. Healing of fractures or faults induced in rock salt formations can prevent the brine flow from contaminating the upper surface or nearby rock formations. The presence of damage in the form of microcracks in salt can alter the structural stability and permeability of salt, affecting the integrity of a repository (Chan et al., 1998b). When cracks are closed, permeability can be reduced by several orders of magnitude. The healing capability of fractures is one of the advantages for rock salt to be used as a host rock for nuclear waste repository in the United States and Germany (Habib and Berest, 1993; Broek and Heilbron, 1998). The healing process of rock salt fractures around an air or gas storage cavern also affects the designed storage capacity and the mechanical stability of the cavern (Katz and Lady, 1976). Numerous studies of fracture healing given in the literature review by Miao et al. (1995) include, for example, the crack healing in geological, the curing concrete, the recovery and recrystallization of metals, and the liquid-phase-enhanced densification of granularly crystalline materials. In rock salt the study on crushed rock salt samples with small amounts water is capable of healing during densification creep processes (Miao et al., 1995). A treatment of damage healing in crushed salt was presented by Miao et al. (1995). In this formulation, a healing surface in the sense of a yield surface in classical plasticity theory is used in conjunction with loading and unloading conditions.

Chan et al. (1994; 1995) and Munson et al. (1999) propose a constitutive formulation for treating damage healing in damaged intact salt, referred to as the multi-mechanism deformation coupled fracture (MDCF) model, which is based on a generalized damage evolution equation that includes both a damage generation term and a healing term. Because, both damage generation and healing are treated, the MDCF model is suitable for treating damage accumulation and healing in disturbed

rock zone in the repository at Waste Isolation Pilot Plant (WIPP) site (Chan et al., 2000).

Fuenkajorn, K. (2007) study the intrinsic variability of rock salt specimens obtained from the Middle and Lower members of the Maha Sarakham formation in the Khorat basin. Prior to the mechanical tests, the types and amount of inclusions were identified by visual examination and after testing by X-ray diffraction and dissolution methods. The uniaxial compressive strength of the specimens linearly increases from 27 MPa to about 40 MPa as the anhydrite content (by weight) increases from 0% (pure halite) to 100% (pure anhydrite). The combined stiffness of the salt and the anhydrite causes an increase of specimen elasticity from 22 GPa (pure salt) to as high as 36 GPa (pure anhydrite). Tensile strengths increase with increasing anhydrite content, particularly when the content is above 60% by weight. Below this limit the anhydrite has an insignificant impact on the specimen tensile strength. The tensile strength of salt crystals can be as high as 2 MPa, whereas that of the inter-crystalline boundaries is 1 MPa. The visco-plasticity increases exponentially with crystal size, as dislocation glide mechanisms become predominant for the specimens comprising large crystals. Salt specimens with fine crystals deform by dislocation climb mechanisms, and hence reduce the specimen's visco-plasticity.

2.3 The effect of temperatures, time and stresses on healing fractures

Jiang et al. (2013) studied the ability of the interface after the salt stress in the laboratory. By making sure that the ultra-sonic technology used to measure the variation of velocity in rock salt. Perform tests under various temperatures are 20, 50

and 70°C. Results showed that when the temperature rises the cracks can be more healed (Figure 2.4). The temperature higher is barely able to accelerate the diffusion of particles in the rock salt and encourage crystallization process repetition.

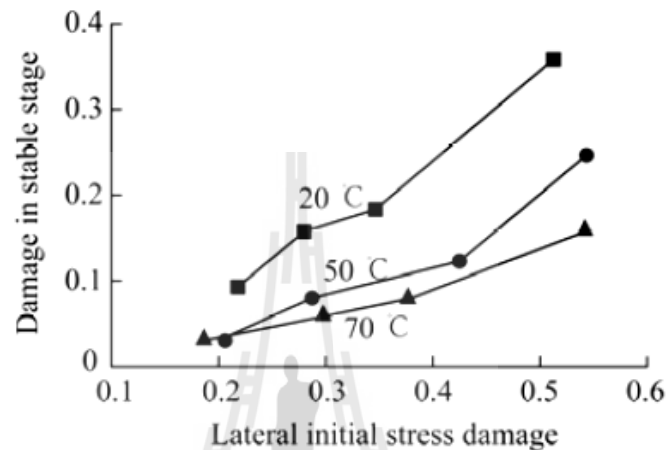


Figure 2.4 Value of lateral initial stress damage vs. value of damage in stable stage

Jiang et al. (2013).

Chen et al. (2013) study the healing properties of rock salt with cracked under the different coordination. This research uses ultrasonic technology to monitor the longitudinal wave velocity variations of stress-damaged rock salts during self-recovery experiments under different recovery conditions. The influences of stress-induced initial damage, temperature, humidity, and oil on the self-recovery of damaged rock salts are analyzed. The wave velocity values of the damaged rock salts increase rapidly during the first 200 h of recovery, and the values gradually increase toward stabilization after 600 h (Figure 2.5). The recovery of damaged rock salts is subjected to higher initial damage stress. Water is important in damage recovery. The

increase in temperature improves damage recovery when water is abundant, but hinders recovery when water evaporates. The presence of residual hydraulic oil blocks the inter-granular role of water and restrains the recovery under triaxial compression. The results indicate that rock salt damage recovery is related to the damage degree, pore pressure, temperature, humidity, and presence of oil due to the sealing integrity of the jacket material.

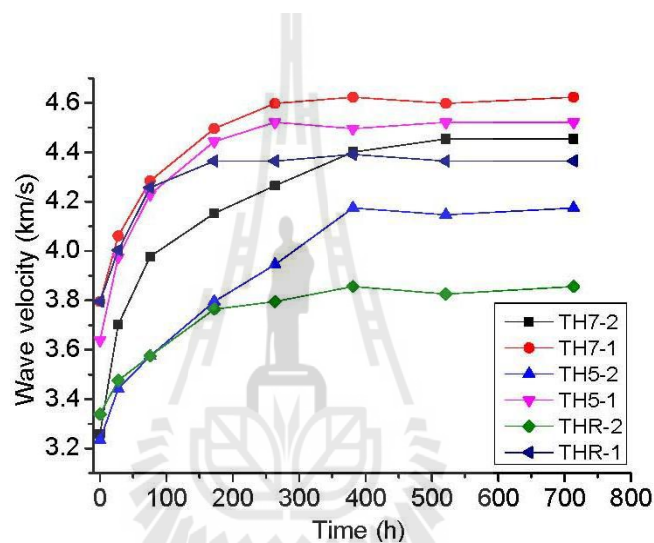


Figure 2.5 Damage variation and time relation curve .The relationship between wave velocity and time curve of rock salts at room temperature, 50 °C and 70 °C (Chen et al., 2013).

Brodsky and Munson (1994) studied the healing in rock salt fractures which is a part of project named “Waste Isolation Pilot Plant” (WIPP). The cylindrical shaped rock salt specimen was stored in a Hock cell under hydrostatic pressure of 0.5 MPa and at temperature of 25°C. The specimen is then compressed in the axial direction to cause a little displacement. After that, the temperature are varied to be 20°C, 46°C and 70°C for each specimen to study the effect from temperature changes. The specimen is loaded

with a strain rate of $1 \times 10^{-6} \text{ sec}^{-1}$. ultrasonic wave velocity test has been also employed to use in conjunction with the test. The derived data have been use as a basic information for comparison with the result from MDCF model created to evaluate healing in anisotropic fracture of rock salt.

Allemandou and Dusseault (1993) have studied the healing of fracture by applying triaxial compressive stress at confining pressure of 2 MPa and constant axial load. The cylindrical shaped rock salt specimen is subjected to the abovementioned stress under constant temperature within several hours. After that the axial stress is changed to be 10, 15, 20, and 25 MPa, respectively. Assessment of closing and healing of fracture from the CAT-scan reveals that healing takes place and voids decrease as stress level increases. Miao et al. (1995) study the healing in crushed salt in less water state and conclude that after the healing takes place, density, inelastic strain, Young's modulus and strength of the crushed salt increase as the time increase.

CHAPTER III

SAMPLE PREPARATION

3.1 Sample preparation

The salt specimens used in this study were drilled from the middle and lower members of the Maha Sarakham Formation in the Khorat Basin, northeast of Thailand. The core specimens were from depths ranging between 250 and 400 m. The drilling was carried out by the Siam Submanee Co., Ltd. The location of cored drill – hole (UTM 47P 0821065/1687136) located in Non Thai district, Nakhon Ratchasima province.

Two types of rock samples are prepared for healing tests: cylindrical and rectangular shaped. The cylindrical shaped specimens will be test under uniaxial (normal) loading. The rectangular shaped specimens will be tests under hydrostatic stresses (Figure 3.1). For healing under uniaxial test, the cores are dry-cut to obtain cylindrical shaped specimens with nominal dimensions of 48 mm diameter and 72 mm length. The average density is measured as $2.13 \pm 0.02 \text{ g/cm}^3$. Two types of fracture are prepared: tension induced fracture and smooth fractures. Specimens with smooth fracture are simulated by using saw-cutting surfaces (Figure 3.2). To obtain the tension-induced fractures, the cylindrical specimens are subjected to point load strength index (Figure 3.3).

For the healing under hydrostatic stresses tests, the rock salts are dry-cut by cutting drive to obtain rectangular shaped with nominal dimensions of 44×44×88 mm

(Figure 3.4). For the healing under hydrostatic stresses tests are applies line loaded parallel to the longitudinal of specimen (Figure 3.5), and are prepared for healing under hydrostatic stresses tests.

The healing tests on salt fracture are made under ambient temperature (25°C) and at high temperature at 70, 150 and 200°C. The aerial percentage of the inclusions is calculated with respect to the total fracture area. These inclusions included all associated and foreign minerals or materials that are not sodium chloride. Table 3.1 shows the specimen dimensions prepared for healing on cylindrical shaped specimen under uniaxial stress at ambient temperature. Table 3.2 show the specimens dimensions prepared for healing under uniaxial tests and elevated temperatures. Table 3.3 show the specimen dimensions prepared for healing under hydrostatic stresses tests and elevated temperatures. The sample preparation and test procedures followed as much as practical the ASTM standard practices (i.e. ASTM D2938, ASTM D3967, ASTM D4543 and ASTM D5731). The average density of salt specimens is $2.13 \pm 0.02 \text{ g/cm}^3$.

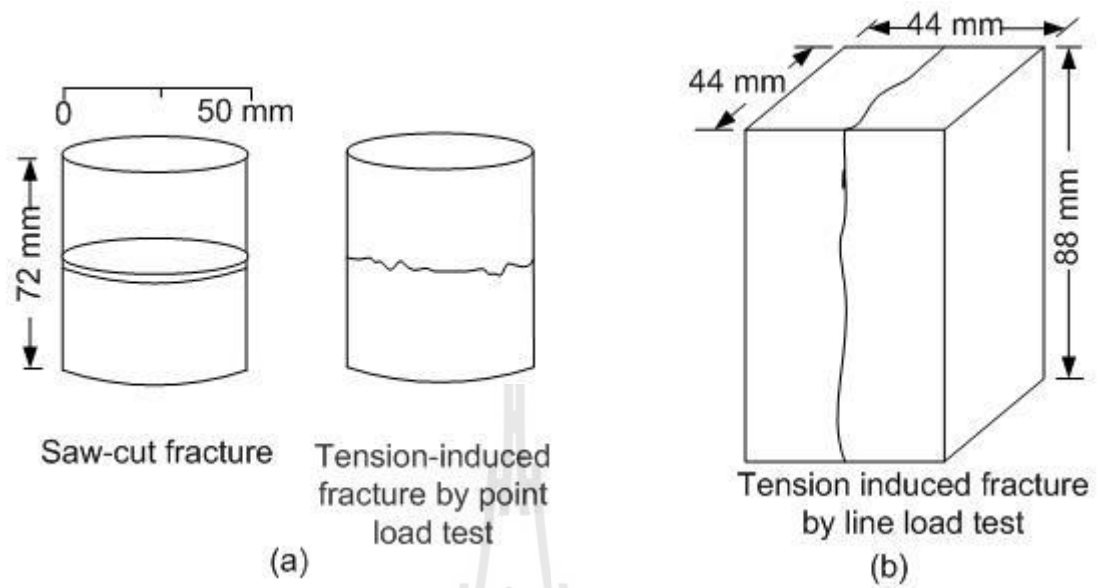


Figure 3.1 Two types of fractures: saw-cut fracture and tension-induced fracture.

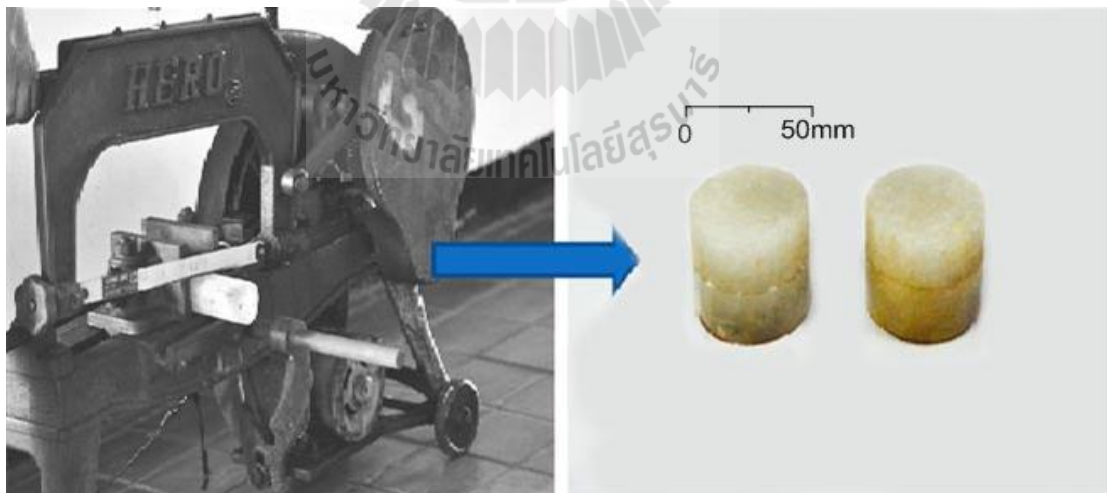


Figure 3.2 Saw-cut fracture specimens are dry-cut by a cutting device.

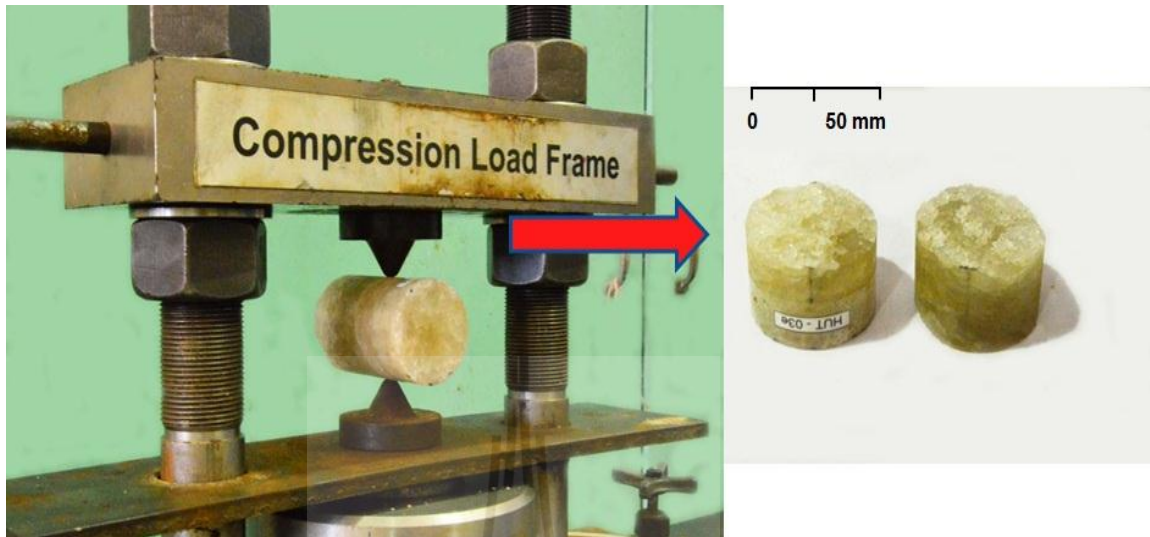


Figure 3.3 Tension induces fractures specimen by point load strength index test.



Figure 3.4 Some rectangular shaped salt specimen with nominal dimensions of 44×44×88 mm in prepared and then it is subjected by line load to induced tensile fracture.

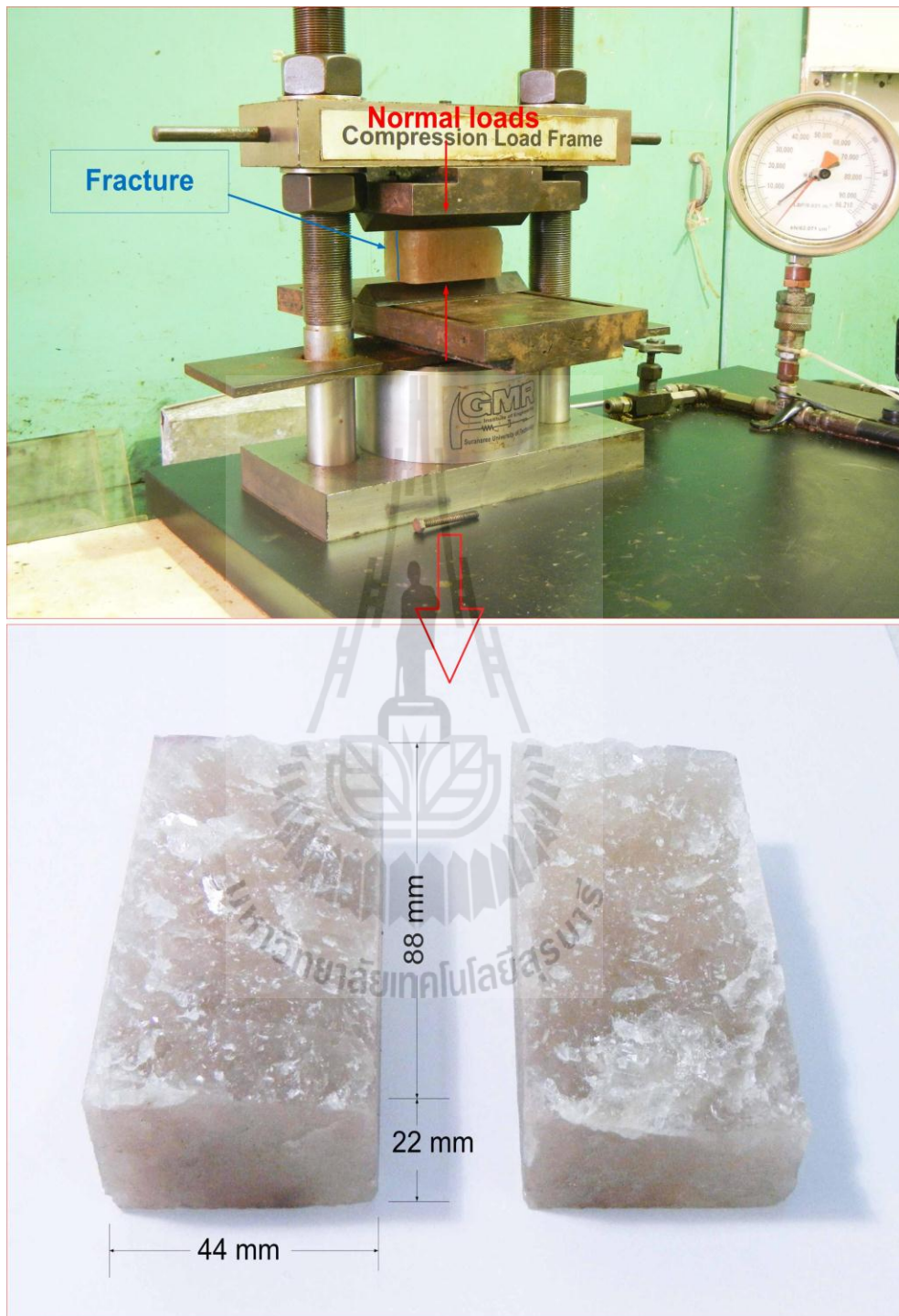


Figure 3.5 Some salt specimen with the tension-induced fracture by line load.

Table 3.1 Cylindrical salt specimens prepared for healing test by subjecting uniaxial loading under ambient temperature.

Specimen No.	Inclusion (%)	Depth (m)	Diameter (mm)	Height (mm)	Density (g/cm ³)
HUT-01e	1	380.25 - 380.45	47.50	72.60	2.15
HUT-10e	5	380.30 - 380.38	47.48	70.95	2.12
HUT-11e	5	375.10 - 375.35	47.44	71.00	2.14
HUT-12e	10	321.00 - 321.20	47.50	70.10	2.14
HUT-13e	15	325.01 - 325.25	47.46	70.60	2.13
HUT-14e	10	325.25 - 325.50	47.52	72.60	2.09
HUT-15e	10	325.50 - 325.80	47.40	72.60	2.14
HUT-16e	5	321.20 - 321.70	47.36	72.60	2.11
HUT-19e	10	313.50 - 313.80	47.46	72.00	2.14
HUT-20e	10	313.50 - 313.80	47.54	72.60	2.16
HUT-21e	5	325.66 - 325.80	47.46	71.00	2.14
HUT-22e	5	276.05 - 276.30	47.50	71.00	2.14
		Average			2.13 ± 0.02

Table 3.2 Cylindrical salt specimens prepared for healing test by subjecting uniaxial loading under elevated temperature at 70, 150 and 200°C.

Specimen No.	Inclusion (%)	Depth (m)	Diameter (mm)	Height (mm)	Density (g/cm ³)
HUT-09e	15	321.20 - 321.70	47.50	70.10	2.14
HUT-08e	5	321.00 - 321.20	47.46	70.60	2.13
HUT-05e	10	325.25 - 325.50	47.52	72.60	2.09
HUT-06e	10	313.50 - 313.90	47.40	72.00	2.14
HUT-07e	5	313.50 - 313.90	47.36	72.00	2.11
HUT-17e	15	313.50 - 313.90	47.46	72.00	2.09
Average					2.13 ± 0.02

Table 3.3 Rectangular salt specimens prepared for healing test by subjecting hydrostatic stresses under ambient temperature and under elevated temperature of 200°C.

Specimen No.	Inclusion (%)	Depth (m)	Area (mm ²)	Height (mm)	Density (g/cm ³)
HCT-01e	5	325.66 - 325.80	44×44	88	2.14
HCT-02e	5	276.05 - 276.30	44×44	88	2.14
Average					2.14

CHAPTER IV

LABORATORY TEST

4.1 Introduction

The objective of this chapter is to explain the healing test procedures and test results. The healing tests are performed by applied the uniaxial stress perpendicular to the tension-induced fracture (by applied point load on the mid-length of cylindrical specimen) and the saw-cut surface fracture (by applied line load along the axial direction of rectangular specimens). The tests are performed the study the affected of elapse time, temperatures, and stresses levels on healing effectiveness. To do this, the specimens are subjected by several of loading condition on fracture and stress levels under ambient temperature and elevated temperature with time. The inclusion on rock specimens is also considered on the healing effectiveness of salt fractures.

4.2 Test methods

The study emphasizes on time, stress, fracture characteristic, and inclusion in rock salt and temperature which theses parameters are the significant factor for the healing of salt fracture. This study excludes other influence factors such as mineral composition and moisture content in rock salt fracture. The healing test of salt fracture can be measured the change of hydraulic and mechanical prosperities of healed fracture. An efficiency of healing fractures cab be evaluated by measured the decrease of hydraulic conductivity of healed fracture by measuring the change in

fracture aperture using ultrasonic techniques (P-wave and S-wave) and measured the change of the mechanical properties using the point load testing on healed fracture for cylindrical shaped specimen and the line load testing on healed fractures for rectangular shaped specimen.

Two test loading conditions are proposed to assess the healing of salt fractures: (1) the healing under uniaxial (normal) stress and (2) the healing under hydrostatic stress. Two types of salt fractures are simulated in the laboratory: (1) saw-cut fracture, (2) the tension-induced fractures by point load test for the cylindrical shaped specimens and by line load test for the rectangular shaped specimens. All fractures are well mated. Table 4.1 summarized the parameters for healing test of salt fracture.

4.2.1 Healing under uniaxial stresses

The dead weights from steel plates are applied on the top of rock sample to induce the uniaxial (or normal) stress on salt fractures (tension induced fracture by point load test and saw-cut fracture). The induced stresses are maintained constant over the prescribed period. Three test series with different test conditions (Table 4.1) have been performed. All tests series are performed under dry conditions. Series I: Healing tests of saw-cut fracture by applying the normal stresses of 0.5 and 2.0 MPa over the prescribed periods (0, 7, 28, and 56 days) under ambient temperature (approximately 25°C) and elevated temperature (200°C).

Series II: Healing tests using tension-induced fracture by point load test under normal stresses of 0.5, 1.0, 1.5 and 2.0 MPa over the prescribed periods (0, 7, 28, and 56 days) at ambient temperature (approximately 25°C). Figure 4.1 shows the test setup for healing test under the uniaxial stress at ambient. The ultra-sonic

Table 4.1 Summarized the parameters for healing test of salt fracture.

Loading Condition	Specimen Shape	Fracture Types	Stress Levels	Time	Temperature (°C)
Uniaxial Stress ($\sigma_1 > 0$ (normal to fracture) and $\sigma_2 = \sigma_3 = 0$)	Cylindrical Shaped Specimen	Saw-cut fracture	0.5 and 2.0 MPa	0, 7, 28, and 56 days	Ambient Temperature and 200°C
		Tension-induced fracture by point loading	0.5, 1.0, 1.5 and 2.0 MPa	0, 7, 28, and 56 days	Ambient Temperature
		Tension-induced fracture by point loading	0.5, 1.0, 1.5 and 2.0 MPa	56 days	25, 70, 150, and 200°C
Hydrostatics Stresses ($\sigma_1 = \sigma_2 = \sigma_3 > 0$)	Rectangular Shaped Specimen	Tension-induced fracture by line loading	5 MPa	0, 6, 12, 24, 48, 72, 120 and 168 hours	Ambient Temperature
			10 MPa	0, 6, 12, 24, 48, 72, 120 and 168 hours	Ambient Temperature
		Tension-induced fracture by line loading	5 MPa	0, 6, 12, 24, 48, 72, 120 and 168 hours	200 °C
			10 MPa	0, 6, 12, 24, 48, 72, 120 and 168 hours	200 °C

waves (P-wave and S-wave) are monitored on the healed tension-induced fractures every 7 days throughout 56 days

Series III: Healing tests using tension-induced fracture by point load test by applying the normal stresses of 0.5, 1.0, 1.5 and 2.0 MPa over the prescribed period (56 days) under elevated temperatures of 25, 70, 150, and 200°C. The heating equipment is used to heat the specimen during healing testing (Figure 4.2). The salt specimens are wrapped with heating tape, foil and insulator throughout the test (Figure 4.3) to maintain constant temperature at prescribed temperatures. The regulator used to controls the temperature on rock samples. The dead weights from steel plates are

applied on the top of rock sample to induce the uniaxial stress on salt fractures. The regulator (right) used to controls the temperature on rock sample (Figure 4.4). The specimen temperatures are assumed to be uniform and constant with time during the healing testing procedure. The ultra-sonic waves (P-wave and S-wave) are monitored same series II

4.2.2 Healing under hydrostatic stresses

The polyaxial load frame (Figure 4.5) is used to apply constant hydrostatic stresses on the rock sample through the cantilever beam with steel plates (Fuenkajorn and Kenkhunthod, 2010). Dead weights are placed on the two lower bars to obtain the pre-defined magnitude of the lateral stresses (confining pressures, σ_3) on the specimens. Simultaneously the axial stress (σ_1) is increased to the same value with lateral stresses to obtain the condition. It is capable of applying confining pressure up to 5 and 10 MPa. In this study, σ_1 (axial stress) and $\sigma_2 = \sigma_3$ (confining pressure) are the same values during healing test under hydrostatic stresses condition.

Two test series with different test conditions (Table 4.1) have been performed on tension induced fracture by line loading of rectangular shaped specimens.

Series I: Healing tests on the tension-induced fracture (rectangular shaped specimens) under hydrostatic stresses condition at ambient temperature. Two hydrostatic stress levels, 5 MPa and 10 MPa, are applied on the rock sample. The healing period are varies from 0.5, 6, 12, 48, 72, 120 and 168 hours. The splitting tensile strength (line load) tests on healed fractures are performed to assess the mechanical performance of the fractures after healing. The rock sample is subjected by hydrostatic stresses at 5 MPa until 0.5 hours, then takes the rock sample out and

repeated the line loading tests to determine the failure load of healed fracture. The same rock sample is repeated use for the healing test at 6, 12, 48, 72, 120 and 168 hours. After that the same rock sample is used for the healing test under hydrostatic stresses of 10 MPa.

Series II: Healing tests on the tension-induced fracture (rectangular shaped specimens) under hydrostatic stresses condition at elevated temperature (200°C). The test procedure and test parameters (hydrostatic stresses level and healing periods) are the same with the previous series but the temperature is changed to 200°C. A digital temperature regulator is used to maintain constant temperature to the specimens up to 200°C. The heater coil is placed on the steel platen (Figure 4.6) and then applied to the four lateral directions of the specimen (Figure 4.7). The electric heating is through a resistor converts electrical energy into heat energy.

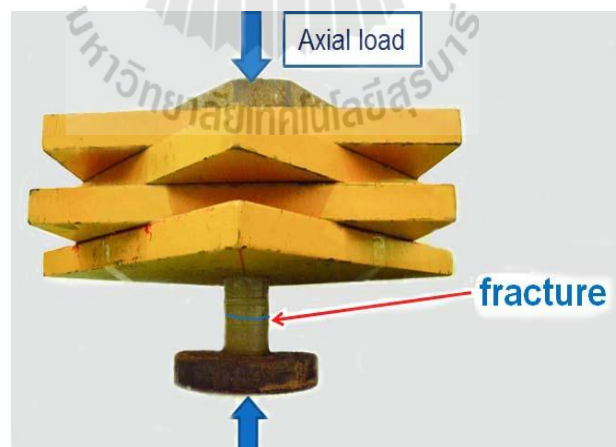


Figure 4.1 Test setup for healing test under the uniaxial stress at ambient temperature. The dead weights from steel plates are applied on the top of rock sample to induce the uniaxial stress on salt fractures.



Figure 4.2 The heating equipment is used to heat the specimen during healing testing. The salt specimens will be wrapped with heating tape, foil and insulator before testing. The regulator (right) used to controls the temperature on rock sample.



Figure 4.3 A salt specimen is wrapped with heating tape, foil and isolator before testing to maintain constant during the test.

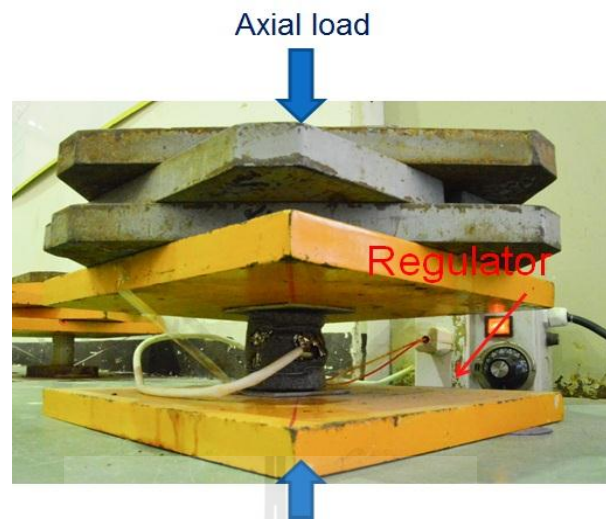


Figure 4.4 Test setup for healing test under the uniaxial stress at elevated temperatures.

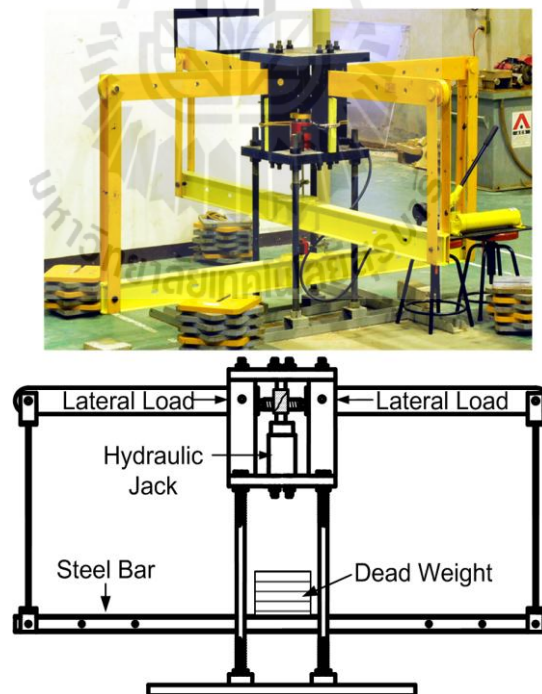


Figure 4.5 Polyaxial load frame (Fuenkajorn and Kenkhunthod, 2010) used to apply constant hydrostatic stresses on the rock sample.

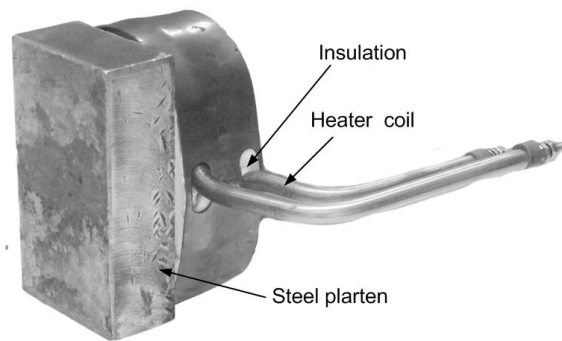


Figure 4.6 Heater coil entwined around steel platen before applied to the rock specimen.

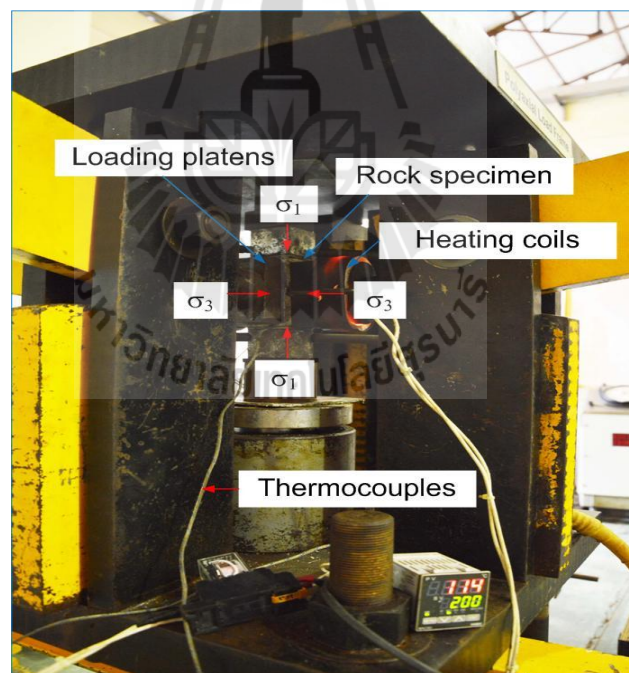


Figure 4.7 Temperatures measured and regulated are made by thermocouples and thermostats.

Electric heating devices use Nichrome (Nickel-Chromium Alloy) wire supported by heat resistant. A thermostat (Figure 4.8) is a component of a control system which senses the temperature of a system so that the system's temperature is maintained near a desired setpoint. The platens are heated by heater coil for 0.5 hours before testing.

4.3 Test results

4.3.1 Healing under uniaxial stresses results

The point load tests on healed fractures are performed to assess the mechanical performance of the fractures after healing (Figure 4.9). The point load tests on the healed fractures have been compared with intact rock salt to determine the healing effectiveness under the test conditions. The point load strength of the healed fracture (I_h) is calculated by dividing the failure load (P_f) by the diameter square (D_e^2):

$$I_h = P_f / D_e^2 \quad (4.1)$$

The healing effectiveness (H_e) of each fracture is defined by the percentage ratio of I_h to I_s (I_s - point load strength index of the intact salt obtained previously from inducing a fracture in the same specimen).

$$H_e = (I_h / I_s) \times 100 \% \quad (4.2)$$

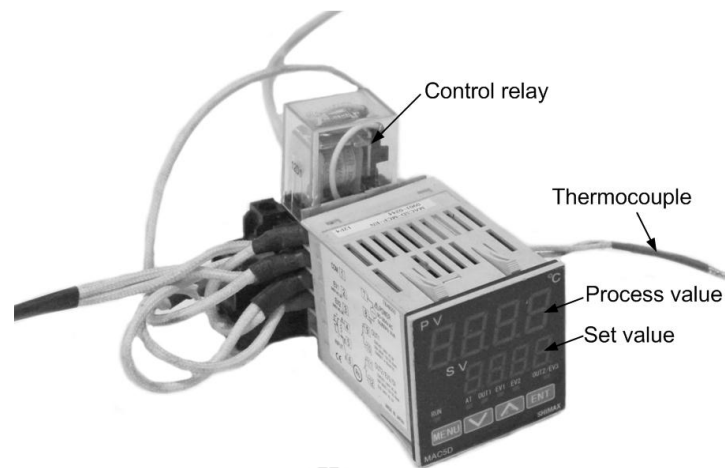


Figure 4.8 Thermostat is a component of a control system which senses the temperature of a system so that the system's temperature is maintained near a desired set point

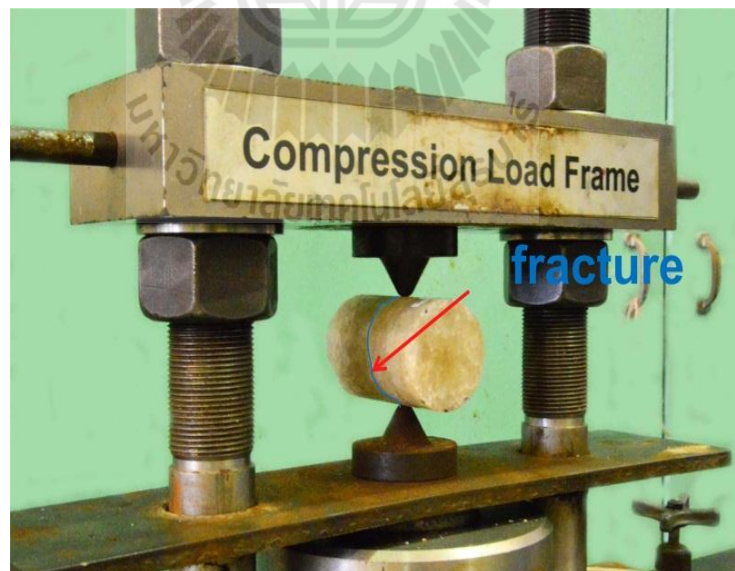


Figure 4.9 The test setup for determining the point load strength index of healed fracture.

Tables 4.2 and 4.3 summarize the test results on the healing effectiveness which they are monitored from salt specimens obtained for the healing test under ambient temperature and under elevated temperatures, respectively.

Table 4.2 Point load strength index test results obtained for the healed tension-induced fracture which tested under uniaxial stresses at ambient room temperature.

Specimen no.	Inclusion (%)	Healing Time (days)	Axial loading (MPa)	Point load strength index		Healing effectiveness H_e (%)
				Intact salt I_s (kPa)	Healed Fracture I_h (kPa)	
HUT-10e	5	56	0.5	8.86	3.98	45.00
HUT-12e	10		1.0	9.97	5.54	55.55
HUT-13e	15		1.5	11.03	6.62	60.00
HUT-01e	1		2.0	8.20	5.54	67.57
HUT-14e	10	28	0.5	8.79	2.20	25.00
HUT-15e	10		1.0	8.79	3.10	35.00
HUT-16e	5		1.5	8.42	3.55	42.11
HUT-11e	5		2.0	8.42	4.21	50.00
HUT-19e	10	7	0.5	8.86	0.44	5.00
HUT-20e	10		1.0	9.31	0.89	9.52
HUT-21e	5		1.5	8.42	1.33	15.79
HUT-22e	5		2.0	8.86	6.20	17.50

Table 4.3 Point load strength index test results obtained for the healed tension-induced fracture which tested under uniaxial stresses at elevated temperature.

Specimen no.	Inclusion (%)	Healing Time (days)	Temp. (°C)	Axial loading (MPa)	Point load strength index		Healing effectiveness H _e (%)
					Intact salt I _s (kPa)	Healed fracture I _h (kPa)	
HUT-10e	5	56	Ambient	0.5	8.86	3.98	45.00
HUT-09e	15	56	70	0.5	10.17	5.31	52.17
HUT-08e	5	56	150	0.5	9.31	5.32	57.14
HUT-05e	10	56	200	0.5	8.13	4.83	59.46
HUT-01e	1	56	Ambient	2.0	8.20	5.54	67.57
HUT-06e	10	56	70	2.0	8.42	5.32	63.16
HUT-07e	5	56	150	2.0	9.31	6.21	66.67
HUT-17e	15	56	200	2.0	8.86	6.21	70.00

The results indicate that the healing effectiveness tends to decrease as the amount of inclusion increases. All the saw-cut fractures remained separable with no healing. The healing effectiveness of tension induced fractures increase with increasing healing time and axial stress (Figure 4.10). The healing test results under uniaxial stresses (Figure 4.11) at elevated temperature shows that the temperatures slightly increase the healing effectiveness.

4.3.2 Wave velocity test results

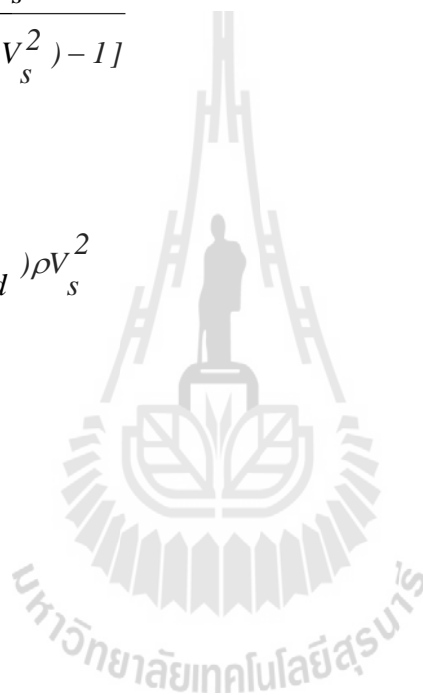
The ultra-sonic wave (P-wave and S-wave) are monitored on intact salt specimens and salt with healed fractures under axial loading for every 7 days throughout 56 days of testing (Figure 4.12).

Table 4.4 summarized wave velocity test results. The wave velocity of the rock salt increases rapidly during the first 7 days, after that the P-wave are slightly increases steadily with time (Figure 4.13). These results indicate that some parts of the

salt fractures are closed or healed, and some parts cannot be recovered or healed. These generally agree with the experimental observations by Chen, et al. (2013). Dynamic elastic modulus and Poisson's ratio of rock salts are also determined using the following relations (pulse velocity measurement – ASTM D2845).

$$v_d = \frac{(V_p^2 / V_s^2) - 2}{2[(V_p^2 / V_s^2) - 1]} \quad (4.3)$$

$$E_d = 2(1 + v_d) \rho V_s^2 \quad (4.4)$$



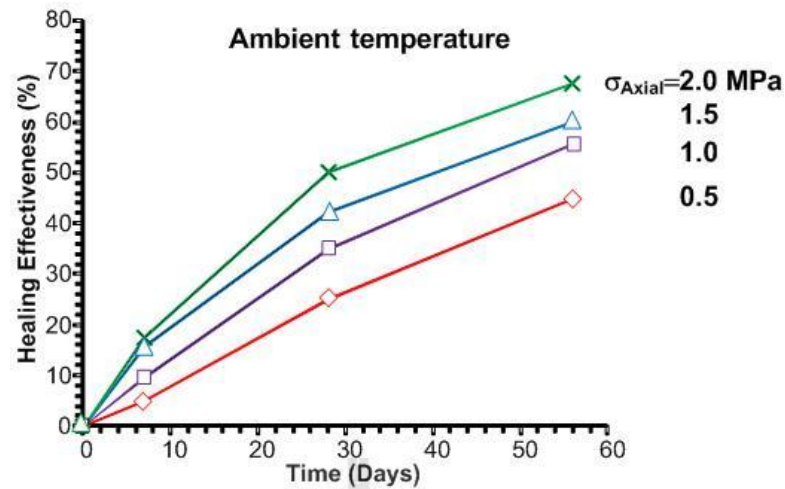


Figure 4.10 Healing effectiveness as a function of healing time obtained from healing test under axial loading on the tension-induced fractures at ambient temperature.

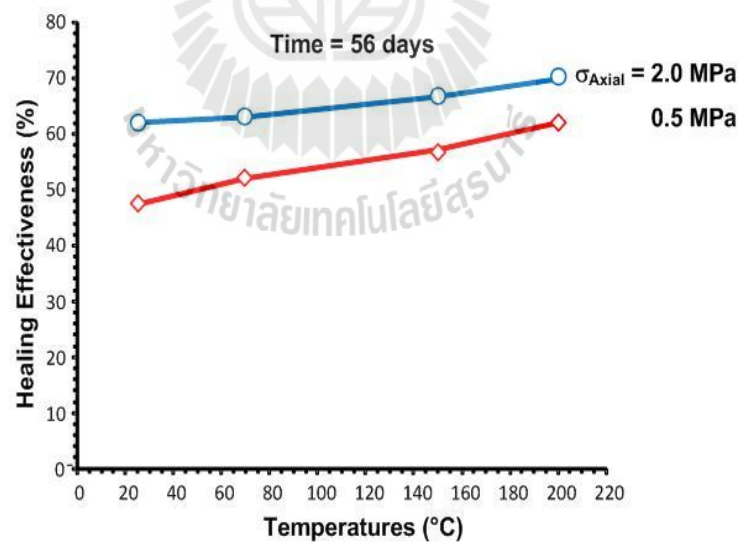


Figure 4.11 Healing effectiveness for 56 days of healing time as a function of temperatures obtained from healing test on the tension-induced fractures under elevated temperature.



Figure 4.12 Wave velocity measurements after fracture healing under uniaxial loading.

Table 4.4 Wave velocity test results for elastic modulus after healing under constant axial stress, elevated temperatures and healing time.

Specimen no.	Inclusion (%)	Time (days)	Axial loading (MPa)	Wave velocity tests		Elastic modulus (GPa)
				P-wave (km/s)	S-wave (km/s)	
HUT-19e	10	7	0.5	3.92	2.10	24.06
HUT-20e	10	7	1.0	3.2	1.64	14.93
HUT-21e	5	7	1.5	3.87	2.12	24.27
HUT-22e	5	7	2.0	3.75	2.10	23.55
HUT-14e	10	28	0.5	4.59	2.42	32.16
HUT-15e	10	28	1.0	5.11	2.6	37.63
HUT-16e	5	28	1.5	4.82	2.55	35.66
HUT-11e	5	28	2.0	4.82	2.55	35.66
HUT-01e	1	56	2.0	5.35	2.7	40.70
HUT-10e	5	56	0.5	4.82	2.68	38.87
HUT-12e	10	56	1.0	5.01	2.54	36.64
HUT-13e	15	56	1.5	5.21	2.72	41.37
HUT-09e	15	56	0.5	5.15	2.68	40.40
HUT-08e	5	56	0.5	5.24	2.75	42.40
HUT-05e	10	56	0.5	5.37	2.72	41.84
HUT-06e	10	56	2.0	5.29	2.74	41.52
HUT-07e	5	56	2.0	5.30	2.72	41.05
HUT-17e	15	56	2.0	5.30	2.74	41.55

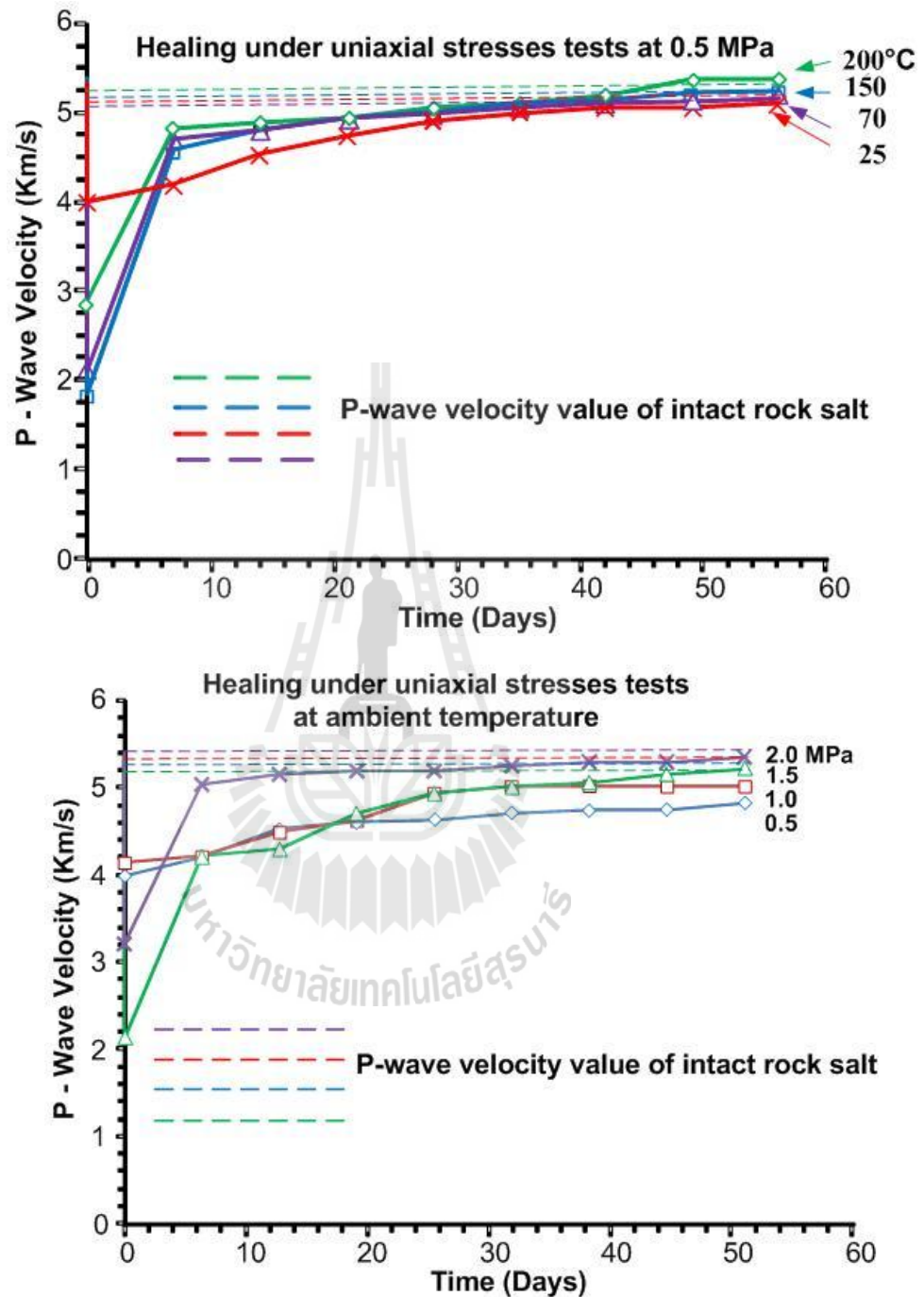


Figure 4.13 P-wave velocities (H_e) as a function of time (t) of tension-induced fractures at uniaxial stresses 0.5 MPa. P-wave velocities (H_e) as a function of time (t) of tension-induced fractures at ambient temperature

4.3.3 Healing under hydrostatic stresses results

The splitting tensile strength (line load) tests on healed fractures are performed to assess the mechanical performance of the fractures after healing. The healing effectiveness (H_e) of each fracture is defined by the percentage ratio of dividing failure load of intact rock (P_i) to dividing failure load after healing time (P_h).

$$H_e = (P_h/P_i) \times 100\% \quad (4.5)$$

Table 4.5 summarizes the healing effectiveness determined for the healing test under hydrostatic stresses. Figure 4.14 shows the healing effectiveness as a function of healing time obtained from healing test under hydrostatic stresses loading (5 and 10 MPa) on tension-induced fractures at ambient temperature and at elevated temperature of 200°C. The healing effectiveness tended to increase with increasing healing time and hydrostatic stresses. Temperatures slightly increase the healing effectiveness (Figure 4.15).

4.4 Discussions and conclusions

The results indicate that the healing effectiveness tends to decrease as the amount of inclusion increases. The healing effectiveness of tension induced fractures increase with increasing healing time and axial stress. Temperatures slightly increase the healing effectiveness. Based on this calculation the dynamic elastic moduli are about 14 to 43 GPa and they tend to increase with stress and healing time increase. The Poisson's ratios of the salt are about 0.28 to 0.35 and they tend to be independent of the time and

temperature. Healing effectiveness determined from healing under hydrostatic stresses conditions are higher than healing under uniaxial stresses condition.

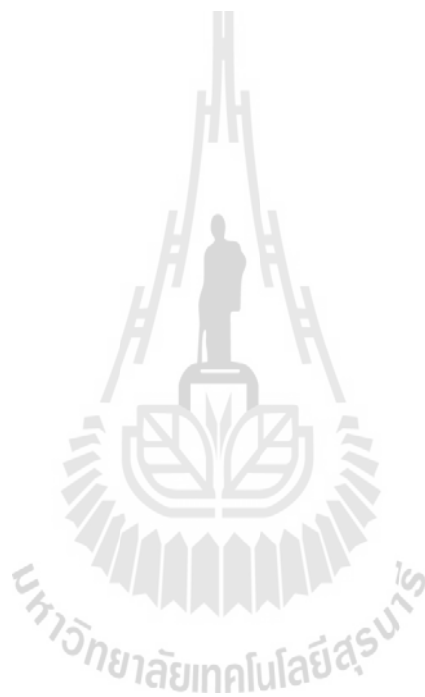


Table 4.5 Healing test under hydrostatic stresses. The fracture healing effectiveness is assessed by elevated temperatures and time.

Specimen No.	Healing time (Hr)	Temp. (°C)	Confining pressure (MPa)	Intact rock failure P_i (kN)	After healing failure P_h (kN)	Healing effectiveness H_e (%)	
HCT-01e	0	Ambient	5	5.50	0.10	1.82	
	6	Ambient	5	5.50	0.90	16.36	
	12	Ambient	5	5.50	1.15	20.91	
	24	Ambient	5	5.50	1.50	27.27	
	48	Ambient	5	5.50	1.90	34.55	
	72	Ambient	5	5.50	2.20	40.00	
	120	Ambient	5	5.50	2.40	43.64	
	168	Ambient	5	5.50	2.55	46.36	
	0	200	5	5.50	0.25	4.55	
	6	200	5	5.50	1.20	21.82	
	12	200	5	5.50	1.50	27.27	
	24	200	5	5.50	1.75	31.82	
	48	200	5	5.50	2.15	39.09	
	72	200	5	5.50	2.50	45.45	
	120	200	5	5.50	2.65	48.18	
	168	200	5	5.50	2.80	50.91	
	HCT-02e	0	Ambient	10	6.60	0.20	3.03
		6	Ambient	10	6.60	2.00	30.30
12		Ambient	10	6.60	2.20	33.33	
24		Ambient	10	6.60	2.50	37.88	
48		Ambient	10	6.60	2.80	42.42	
72		Ambient	10	6.60	3.10	46.97	
120		Ambient	10	6.60	3.30	50.00	
168		Ambient	10	6.60	3.60	54.55	
0		200	10	6.60	0.55	8.33	
6		200	10	6.60	2.55	38.64	
12		200	10	6.60	2.70	40.91	
24		200	10	6.60	2.85	43.18	
48		200	10	6.60	3.10	46.97	
72		200	10	6.60	3.40	51.52	
120		200	10	6.60	3.80	57.58	
168		200	10	6.60	4.10	62.12	

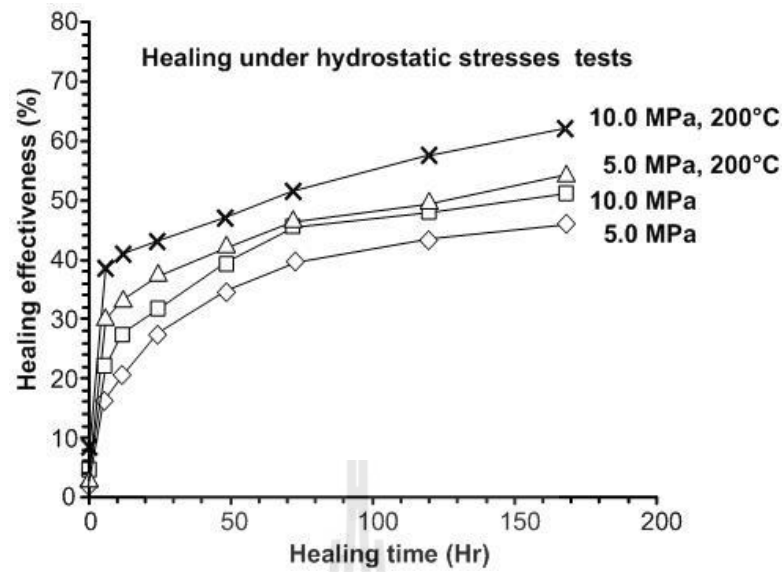


Figure 4.14 Healing effectiveness as a function of healing time obtained from healing test under hydrostatic stresses loading (5 and 10 MPa) at ambient temperature and at elevated temperature of 200°C.

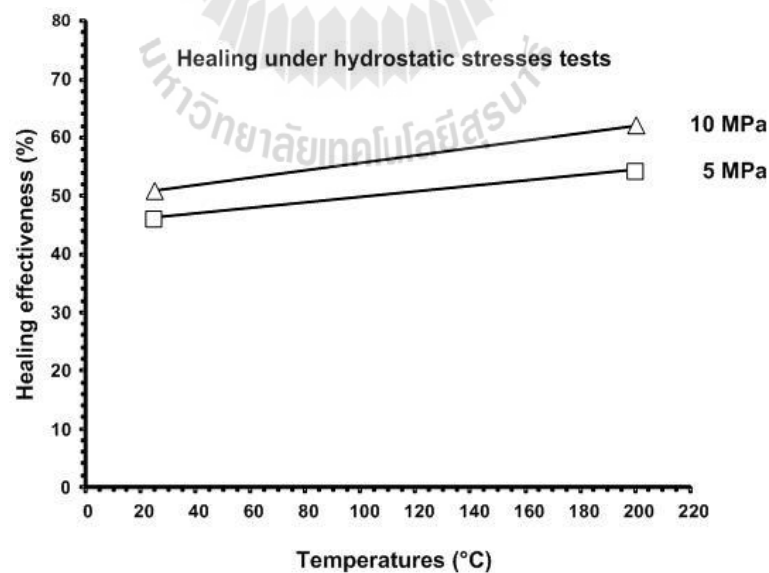


Figure 4.15 Healing effectiveness (at 168 hours) as a function of temperatures obtained from healing test under hydrostatic stress loading of 5 and 10 MPa.

CHAPTER V

DEVELOPMENT OF HEALING EFFECTIVENESS

CRITERIA

5.1 Objectives

This chapter describes the development the mathematical relationship between the healing effectiveness as a function of stresses, time and temperatures. These mathematical relationships can be used to predict the mechanical properties of healed fractures around the salt opening under such stresses and temperature for the proper time. These empirical equations based on the laboratory testing results obtaining under various testing conditions. The stresses on the fractures for healing tests are limited as follows; they cannot exceed the elastic point of intact rock (approximately 30% of the uniaxial compressive strength of intact salt). This is due to the new micro-crack will be induced in the rock sample. The regression analyses of the proposed healing effectiveness equations are attempted by using the IBM SPSS Statistics 19 (Wendai, 2000) to determine healing effectiveness parameters.

5.2 Healing effectiveness criterion

5.2.1 Healing under uniaxial stresses criterion

An empirical equation proposed here use to predict the healing effectiveness of tension induced fracture of rock salt as a functions of various stresses and time under constant temperature of ambient temperature (25°C).

$$H_e = 100 - [100 / (1 + \alpha \sigma_{\text{axial}}^\beta t^\delta)] \quad (\%) \quad (5.1)$$

Where “ H_e ” is the healing effectiveness of rock salt (%), “ σ_{axial} ” is axial stresses conditions of healing (MPa), “ t ” is the healing time (Days), α , β and δ are empirical constants. This equation is suitable for low axial stress (less than 10% of strength of intact rock salt) conditions. The temperatures should be ranging between 15 to 35°C.

For the Maha Sarakham salt, the empirical constants in equation (5.1) are defined by the regression analysis as: $\sigma_{\text{axial}} = 0.5, 1.0, 1.5$ and 2.0 MPa; $t = 0, 7, 28$ and 56 days. All tests specimens tested in ambient temperature (25°C). The empirical constants can be calculated as $\alpha = 0.014$; $\beta = 0.704$; $\delta = 1.117$. Regression analysis of equation (5.1) by using the test data is performed to determine the healing effectiveness parameters (Table 5.1). Good correlation is obtained ($R^2 = 0.998$). Figure 5.1 compares the test results with the back predictions from the proposed equation.

Table 5.1 Empirical constants obtained for the healing of salt fracture under uniaxial stresses conditions at ambient temperature (25°C).

Parameters	Unit	Values	R^2
α	-	0.014	0.998
β	-	0.704	
δ	-	1.117	

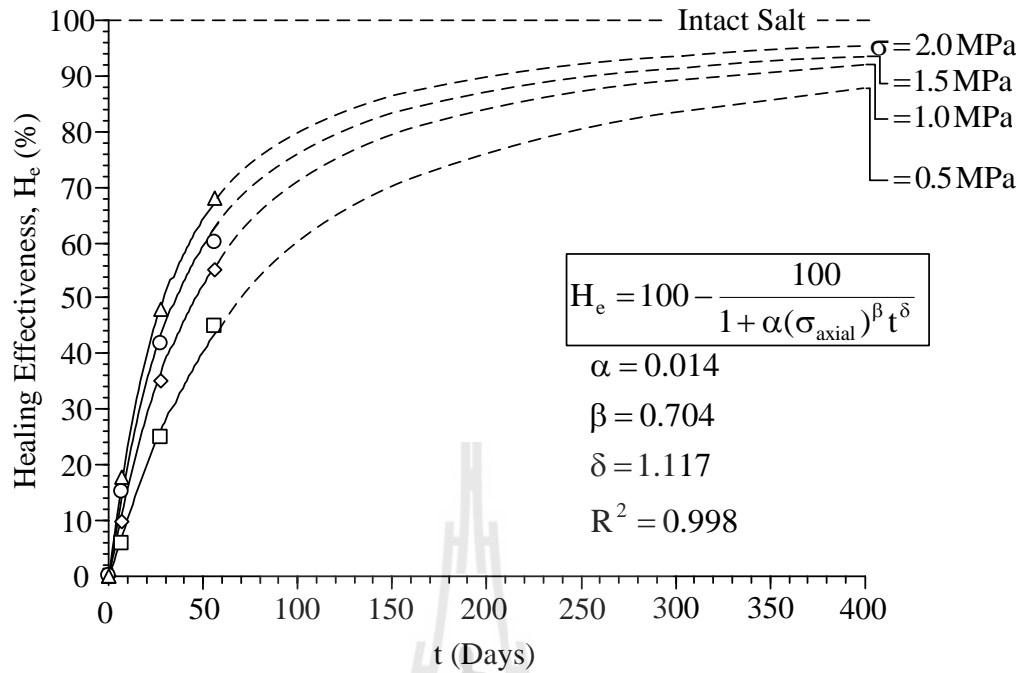


Figure 5.1 Healing under uniaxial tests as a function of healing time: test results (points), regression analysis results (solid lines) and prediction (dashed line).

5.2.2 Healing under hydrostatic stresses criterion

An empirical equation proposed here use to predict the healing effectiveness of tension induced fracture of rock salt as a functions of various stresses and time. This conditions tests in ambient temperature:

$$H_e = 100 - [100 / (1 + \kappa \sigma_{\text{Hydrostatic}}^{\omega} t^{\eta} T^{\lambda})] \quad (\%) \quad (5.2)$$

Where “ H_e ” is the healing effectiveness of rock salt (%), “ $\sigma_{\text{hydrostatic}}$ ” is hydrostatic stresses conditions of healing (MPa), “ t ” is the healing time (Hour), κ , ω , η and λ are

empirical constants. For the Maha Sarakham salt the empirical constants in equation (5.2) are defined by the regression analysis as: $\sigma_{\text{hydrostatic}} = 5$ and 10 MPa; $t = 0, 6, 12, 24, 48, 72, 120$ and 168 Hour; $T =$ Ambient temperature. The empirical constants can be calculated as $\kappa = 0.024$; $\omega = 0.324$; $\eta = 0.426$; $\lambda = 0.279$. Good correlation is obtained ($R^2 = 0.988$). Figure 5.2 compares the test results with the back predictions from the proposed equation. Regression analysis of equation (5.2) by using the test data is performed to determine the healing effectiveness parameters (Table 5.2).

This equation is suitable for hydrostatic stresses (less than 30% and more than 5% of strength of intact rock salt) conditions. The equation is more reliable, healing time should be between 1 to 170 hours, temperatures should be between 15 to 35°C.

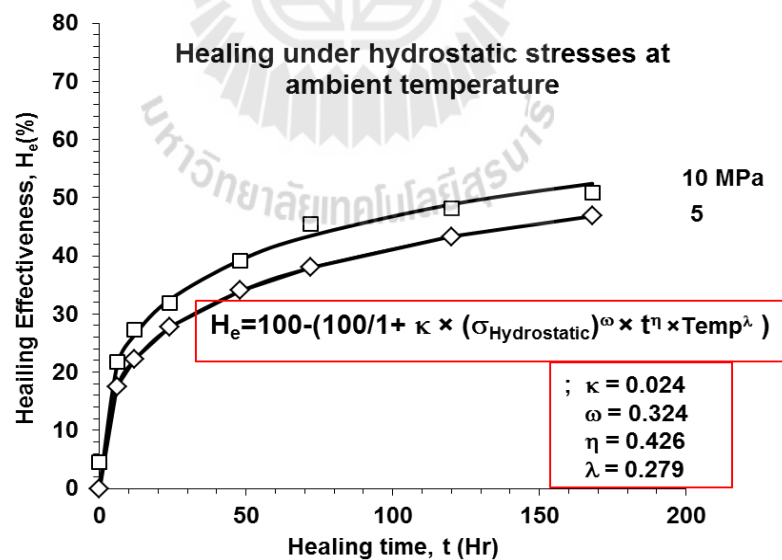


Figure 5.2 Healing under hydrostatic stresses tests at ambient temperature as a function of healing time, test results (points) and back predictions (lines).

Table 5.2 Empirical constants obtained for the healing of salt fracture under hydrostatic stresses conditions at ambient temperature (25°C).

Parameters	Unit	Values	R ²
κ	-	0.024	0.988
ω	-	0.324	
η	-	0.426	
λ	-	0.279	

An empirical equation proposed here use to predict the healing effectiveness of tension induced fracture of rock salt as a functions of various stresses time and temperatures.

$$H_e = 100 - [100 / (1 + \psi \sigma_{\text{Hydrostatic}}^{\phi} t^{\zeta} T^{\xi})] \quad (\%) \quad (5.3)$$

Where “H_e” is the healing effectiveness of rock salt (%), “σ_{hydrostatic}” is hydrostatic stresses conditions of healing (MPa), “t” is the healing time (Hour), “T” is temperatures(°C), ψ, φ, ζ and ξ are empirical constants. For the Maha Sarakham salt the empirical constants in equation (5.3) are defined by the regression analysis as: σ_{hydrostatic}= 5 and 10 MPa; t = 0, 6, 12, 24, 48, 72, 120 and 168 Hour; Temperature is 200°C. The empirical constants can be calculated as ψ = 0.024; φ = 0.385; ζ = 0.293; ξ = 0.327. Good correlation is obtained (R² = 0.969). Figure 5.3 compares the test results with the back predictions from the proposed equation. Regression analysis of equation (5.3) by using the test data is performed to determine the healing effectiveness parameters (Table 5.3).

This equation is suitable for hydrostatic stresses (less than 30% and more than 5% of strength of intact rock salt) conditions. The equation is more reliable, healing time should be between 1 to 170 hours, temperatures should be 200°C.

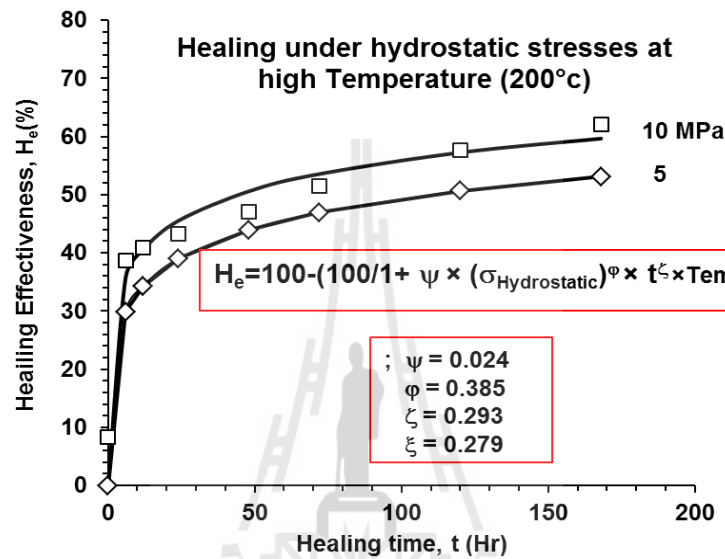


Figure 5.3 Healing under hydrostatic stresses tests at high temperature as a function of healing time, test results (points) and back predictions (lines).

Table 5.3 Empirical constants obtained for the healing of salt fracture under hydrostatic stresses conditions at high temperature (25°C).

Parameters	Unit	Values	R ²
ψ	-	0.024	0.969
ϕ	-	0.385	
ζ	-	0.293	
ξ	-	0.327	

5.3 Applications

The proposed equations are further efforts to predict the healing effective of salt fracture around the salt cavern in the compressed-air energy storage (CAES) technology. The cylindrical cavern with haft-spherical shape at the top and the bottom with 50 m-diameter and 150-m height is assumed for CAES. The cavern roof is designed at 600-m depth to the cavern roof. The cavern is subjected by the pressure fluctuation, at minimum and maximum pressures of 20% and 90% of in-situ stresses at cavern roof. The density gradient of overburden rock and salt are assume to be 0.025 and 0.021 MPa/m, respectively (Phueakphum, 2003). Under this operation, the fractures are induced in salt around the cavern (Figure 5.4) under minimum pressure. Under maximum pressure the induced fractures are subjected under high stresses condition.

Case I: Under hydrostatic conditions, the vertical stress (σ_v), the tangential and radial stresses (σ_θ and σ_r) can be calculated by using the following equations (Brady and Brown, 2006);

$$\sigma_v = \Sigma(\rho gh) \quad \text{MPa} \quad (5.4)$$

$$\sigma_\theta = \frac{P_1 + P_2}{2} \left(1 + \frac{a^2}{r^2} \right) - \frac{P_1 - P_2}{2} \left(1 + \frac{3a^4}{r^4} \right) \cdot \cos 2\theta - P_i \left(\frac{a^2}{r^2} \right) \quad \text{MPa} \quad (5.5)$$

$$\sigma_r = \frac{P_1 + P_2}{2} \left(1 - \frac{a^2}{r^2} \right) + \frac{P_1 - P_2}{2} \left(1 - \frac{4a^4}{r^2} + \frac{3a^4}{r^4} \right) \cdot \cos 2\theta + P_i \left(\frac{a^2}{r^2} \right) \quad \text{MPa} \quad (5.6)$$

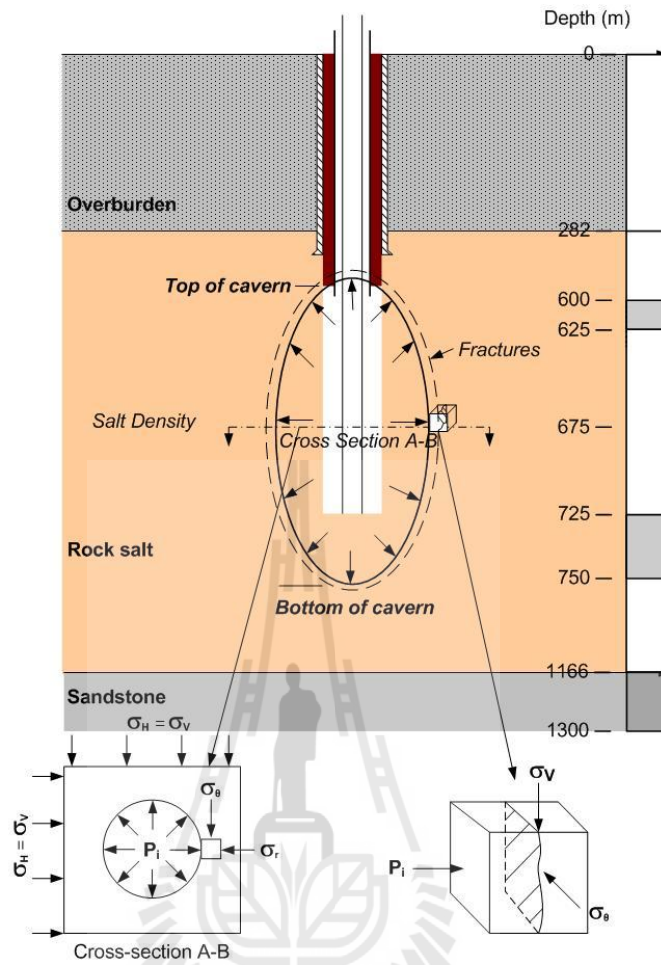


Figure 5.4 Stresses around salt cavern and induced fracture during minimum pressure of operation.

Where “ σ_θ ” is the tangential stress (in MPa), “ σ_r ” is the radial stress (in MPa), “ P_1 ” and “ P_2 ” horizontal stresses (in MPa), “ r ” is the distance from the center of cavern to the periphery of the cavern, “ a ” is radian of the cavern, “ θ ” is the angle between of “ P_1 ” and “ r ”, “ P_i ” is internal pressure (MPa). Under hydrostatic conditions, $P_1 = P_2 = P$ and considering the stresses condition at cavern boundary ($r = a$), the Equations (5.5) and (5.6) are as follows;

$$\sigma_{\theta} = 2P - P_i \quad \text{MPa} \quad (5.5)$$

$$\sigma_r = P_i \quad \text{MPa} \quad (5.6)$$

The vertical stress ($\sigma_v = \sigma_h$) at mid-height (675 m depth) of salt cavern can be calculated as 15.3 MPa. The stress at cavern roof (600 m depth) is about 13.7 MPa. Under maximum pressure (90% of in-situ stress at cavern roof) which P_i is proximally 12.4 MPa and $P = 15.0$ MPa. By using Equations (5.4) and (5.5) σ_{θ} and σ_r can be calculated as 17.6 and 12.4 MPa, respectively. This can be defined that $\sigma_1 = \sigma_{\theta} = 17.6$ MPa, $\sigma_2 = \sigma_v = 15.3$ MPa and $\sigma_3 = \sigma_r = 12.4$ MPa. At the mid-height of cavern, the stress is approximately 15.0 MPa, If the cavern is subjected under these stress and temperature conditions within 1 days, by using Equation (5.2), this condition is considered only the normal stress from internal pressure and the fractured are healed under 25°C. The mechanical properties of healed fracture can be recovered approximately 35% ($100 - (100 / (1 + 0.024 \times 24^{0.426} \times 15^{0.324} \times 25^{0.279}))$) of intact rock salt.

By using Equation (5.1), this condition is considered only the normal stress from internal pressure and the fractured are healed at 25°C. The mechanical properties of healed fracture can be recovered approximately 8% ($100 - (100 / (1 + 0.014 \times 12.4^{0.704} \times 1^{1.117}))$) of intact rock salt. The results show that the fracture healing under hydrostatic stress condition is higher than under only normal stress condition. The real stress condition the stress is under between hydrostatic stress and

uniaxial stress conditions. It can be concluded that the healing effectiveness should not less than 8% and not over than 41% under real condition.

Case II: Considering under condition ($r \neq a$): Under hydrostatic conditions, the vertical stress (σ_v), the tangential and radial stresses (σ_θ and σ_r) can be calculated by using the following case I; The variable ratio (r/a) are increase every 0.1 times until five times. Figure 5.5 and 5.6 compare the variable (r / a) with healing effectiveness

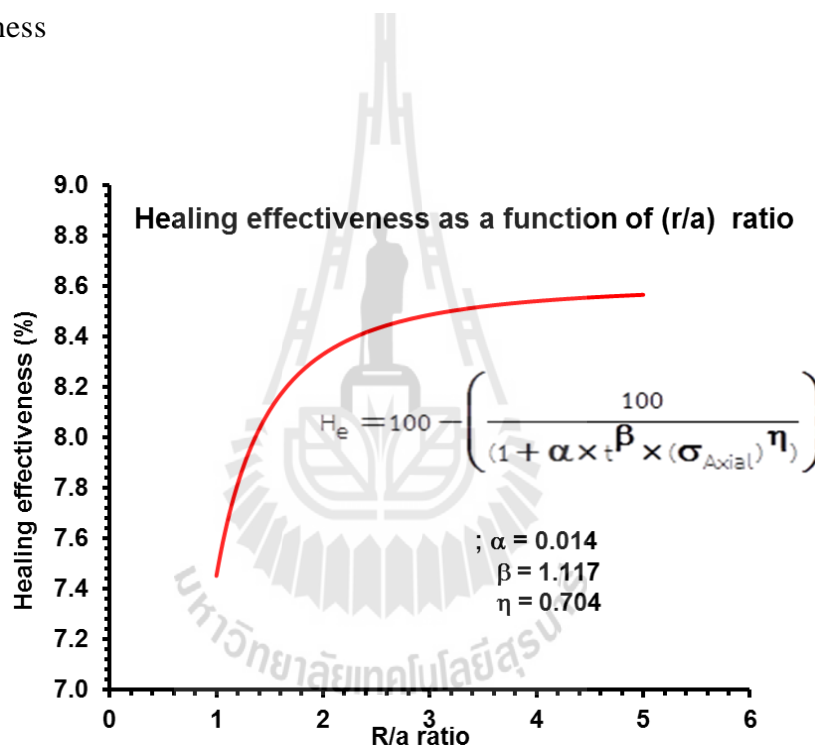


Figure 5.5 Healing effectiveness as a function of the variable of (r/a) ratio. This figure used the equation 5.1 for predicted healing effectiveness.

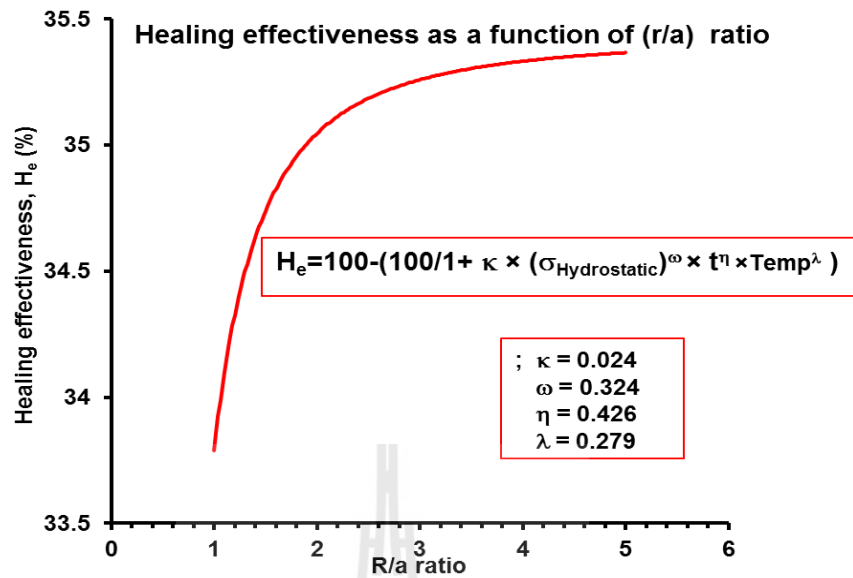


Figure 5.6 Healing effectiveness as a function of the variable of (r/a) ratio. This figure used the equation 5.2 for predicted healing effectiveness.

The results indicated that the healing effectiveness increase rapidly for radial (r) extend about 1-2 times of cavern radius (a) and then to constant after the r/a ratio in the last stage (2-5 times), when the r/a ratio are increase the healing effectiveness slightly increase after that healing effectiveness increase very few when comparing with the variable ratio (r/a)

5.4 Discussions of the results

The empirical equations proposed here based on the laboratory testing results obtaining under various testing conditions. The regression analyses are attempted by using the IBM SPSS Statistics 19. Good correlations are obtained for both the

healing effectiveness formulas under uniaxial conditions. The back predictions results agree with the testing results which can be concluded that the proposed empirical equations were reliable and suitable for the healing effectiveness predictions under such stresses and time. However, the proposed formulas are not well predicted for only the short healing time (less than 7 days for healing under uniaxial stresses conditions). From the example case (the cavern for CAES technology) show that the mechanical properties of healed fracture can be recovered more than 8% under real condition.

The stresses on the fractures for healing tests are limited as follows; they cannot exceed the elastic point of intact rock (approximately 30% of the uniaxial compressive strength of intact salt). This is due to the new micro-crack will be induced in the rock sample. It can be concluded that the proposed formula developed here are reliable and suitable for the healing effectiveness predictions only under low stresses (not exceed the elastic region of intact rock).

CHAPTER VI

DISCUSSIONS, CONCLUSIONS AND RECOMMENDATIONS FOR FUTURE STUDIES

6.1 Discussions

This section discusses the key issues relevance to the reliability of the test schemes and the adequacies of the test results. Comparisons of the results and findings from this study with those obtained elsewhere under similar test conditions have also been made.

Series I: This explains why the saw-cut fractures cannot be effectively healed under the test conditions used here. It is postulated that healing of a fracture can be enhanced by the purity of the halite crystals on the opposite sides of the fracture. This is supported by the fact that the cleavage planes inside the salt crystal are purer than the inter-crystalline boundaries, and purer than the saw-cut surfaces. These artificial surfaces could be contaminated during the preparation process. Roughness caused by a saw-cut and other inclusion may be covering the artificial surface. However, in this test conditions use here the temperatures to help facilitate the healing effectiveness. But from tests found that even applies temperatures under elevated temperatures (70, 150 and 200°C) healing effectiveness of saw-cut fractures not occurred. To heal a saw-cut fracture, a much axial stress (more than 10% of strength and not over than 30% of strength) and time than those used here may be required for closed aperture between inter-crystalline boundaries of saw-cut fractures for Increase the possibility

of healing effectiveness. For the fractures formed by separation of inter-crystalline boundaries, healing will not be easily achieved. In particular, if the fracture surface is coated with any inclusions, healing will not occur.

Series II: The healing of salt fractures depends largely on the origin of the fractures. If a fracture is formed by separation or splitting of salt crystals (tension induce fracture), it can be easily healed even under relatively low stress for a short period. The splitting failure of salt crystals occurs by a separation of cleavage planes, which means that healing is likely to occur if the salt crystals on both sides of the cleavage plane return to their original position.

Series III: It is not clear from the experimental results fractures under high temperature can be healed more than those under ambient temperatures (from figure 4.11) it can be seen that temperatures as affected slightly with healing effectiveness as a compared with effect of stresses and time. Since, higher temperatures adversely affect humidity in open systems and the healing effect of increased temperature is counteracted by loss of necessary water as the rock dries out.

After the tension induced fracture of rock salt are tests by healed under uniaxial stresses under certain conditions of time, temperatures and stresses, the fractures can be restored, but not to its full or initial state. P-wave velocity values of rock salt increase rapidly with healing time at 7 days, and increase slowly after 7 days until the values stabilize. Generally, the wave velocity of rock salt will tend to stabilize after 21 days of healing tests. This phenomenon indicates that some parts of the internal fractures are closed or healed, and some parts of the larger fractures cannot be recovered by fractures closure or recrystallization. Whereas specimen fractures appear with a certain amount of closure characterized by indirect wave

velocity increase and accompanied by a small amount of grain growth. It also explains the rapid increase of the wave velocity at 7 days after tests. Maximum of P-wave velocities recovery healing is observed on the initial phase(7 days) under the four baking temperatures (Figure 4.13), which is mainly ascribed to the specimens which are damaged by tension induced fractures (part of the P-wave velocity recovers slowly after unloading) and at the beginning of the recovery period; temperature does not affect recovery, whereas initial stresses and time can induce a small healing.

Fracture healing under hydrostatic stresses has an advantage over that healing under axial stresses, in term of the maximum applied stresses. The applied stress is limited by the compressive strength of rock salt. The maximum axial stress used here is therefore limited to 2 MPa or about 5% of the strength. This is primarily to prevent the initiation of fractures in the intact salt. For the hydrostatic stresses, the specimen can subject to hydrostatic as high as 10 MPa. Fracture healing under hydrostatic stresses has more efficiency than those healing under axial stresses.

For the healing assessment method, a direct tension test could be used to minimize the impact of the stress gradient induced along the fracture plane. From the results obtained here, it can be postulated that under preferable conditions (stress state, time, purity and temperature), a complete healing of salt fractures is possible.

6.2 Conclusions

All objectives and requirements of this study have been met. The results of the laboratory testing and analyses can be concluded as follows:

Series I: Healing tests of saw-cut fracture by applied the normal stresses of 0.5 and 2.0 MPa over the prescribed periods (0, 7, 28, and 56 days) under ambient temperature (approximately 25°C) and elevated temperature (200°C). The results indicated that the saw-cut fractures remained separable with no healing these agree with the experimental results on rock salt performed by (Fuenkajorn and Phueakphum, 2011).

Series II: Healing tests used tension-induced fracture by point load test under normal stresses of 0.5, 1.0, 1.5 and 2.0 MPa over the prescribed periods (0, 7, 28, and 56 days) at ambient temperature (approximately 25°C). The testing is assumed to be under isothermal conditions (constant temperature and constant stresses with time during loading). The results indicate that the healing effectiveness tends to decrease as the amount of inclusion increases. The healing effectiveness increase with increasing stresses and time these agree with the experimental results on rock salt performed by (Fuenkajorn and Phueakphum, 2011).

Series III: Healing tests used tension-induced fracture by point load test by applied the normal stresses of 0.5, 1.0, 1.5 and 2.0 MPa over the prescribed period (56 days) under elevated temperatures of 25, 70, 150, and 200°C. The results indicate that temperatures can induce the slight increase of the healing effectiveness. This is a conclusion drawn by Chen, et al. (2013), who found that the temperatures have a large effect on healing effectiveness because this may be due to that they tested micro cracks and this study is concentration tested on fractures. The effectiveness of healing is sensitive to the both axial stress and healing time more than to the temperature (within the range up to 200°C.)

Based on this calculation the elastic modulus of the salt appears to increase with stress and healing time increase. It ranges from 14 to 43 GPa. The Poisson's ratio of the salt range from 0.28 to 0.35 and tend to be independent of the time and temperature.

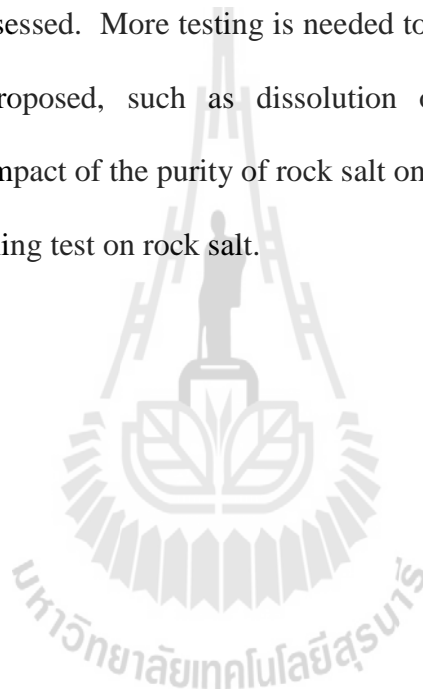
The wave velocity of the rock salt increases rapidly during the first 7 days, and after that the P-wave are slightly increases steadily with time (Figure 4.13). These results indicate that some parts of the salt fractures are closed or healed, and some parts cannot be recovered or healed. These generally agree with both the experimental observations by Chen, et al. (2013) and Jiang, et al. (2013). Actually the temperature higher is barely able to accelerate the diffusion of particles in the rock salt and encourage crystallization process repetition in during the first 7 days of laboratory tests.

For healing under hydrostatic stresses tests are applies hydrostatic stresses of 5 and 10 MPa. The testing temperatures are maintained constant of ambient and 200°C. The results indicate that healing effectiveness tended to increase with increasing healing time and hydrostatic stresses. The healing effectiveness is slightly affected with temperatures (Figure 4.15). The orientations of sample in used here for healing under hydrostatic tests are not effect to healing effectiveness.

The splitting failure of salt crystals occurs by separation of cleavage planes. This means that healing is effective if the salt crystals on both sides cleavage plane return to their original position.

6.3 Recommendations for future studies

The uncertainties and inadequacies of the research investigation and results discussed above lead to the recommendations for further studies. The test specimens here are relatively small. Testing on larger specimens is desirable to confirm the research findings. Verification of the healing effectiveness test proposed concept should be tested under a wider range of salt from other sources. The effect of moisture should be assessed. More testing is needed to confirm the applicability and limitations of the proposed, such as dissolution of rock salt under ambient temperature test, the impact of the purity of rock salt on the healing effectiveness test, and triaxial cyclic healing test on rock salt.



REFERENCES

- Allemandou, X. and Dusseault, M.B. (1993). Healing processes and transient creep of salt rock. In **Geotechnical engineering of hard soils-soft rocks**. Balkema: Rotterdam, Netherlands. pp. 1581–1590.
- ASTM D3967-81. (1981). Standard test method for splitting tensile strength of intact rock core specimens. In **Annual book of ASTM standards** (vol. 40.08). Philadelphia: American Society for Testing and Materials.
- ASTM D4543-85. (1985). Standard practice for preparing rock core specimens and determining dimensional and shape tolerances. In **Annual book of ASTM standards**(vol. 40.08). Philadelphia: American Society for Testing and Materials.
- ASTM D5731-95. (1995). Standard test method for determination of the point load strength index of rock. In **Annual book of ASTM standards** (vol. 40.08). Philadelphia: American Society for Testing and Materials.
- ASTM D2938-79. (1979). Standard test method for unconfined compressive strength of intact rock core specimens. In **Annual book of ASTM standards** (vol. 40.08). Philadelphia: American Society for Testing and Materials.
- Brady, B.G.H. and E.T. Brown (2006). **Rock Mechanics for Underground Mining**. (3rd edition) springer. pp. 626.
- Brodsky, N.S. and Munson, D.E. (1994). Thermo-mechanical damage recovery parameters for rock salt from WIPP, Rock Mechanics: Models and Measurements, Challenges from Industry. In **Proceedings of the First North**

- American Rock Mechanics Symposium** (pp.731-740). University of Texas at Austin. Balkema: Rotterdam, Austin.
- Chan, K.S., Munson, D.E., Fossum, A.F., and Bodner, S.R. (1998b). A Constitutive Model for Representing Coupled Creep, Fracture and healing in rock salt. In **Proceeding of the Fourth Conference on the Mechanical Behavior of salt.** (pp. 211-234) June 17-18, 1996. The Pennsylvania State University, Germany.
- Chan, K.S., Bodner, S.R. and Munson, D.E. (2001). Recovery and healing of damage in WIPP salt. **International Journal of Damage Mechanics.** 10:347-375.
- Chen, J., Ren, S., Yang, C., Jiang, D. and Li, L. (2013). Self-Healing Characteristics of Damage Rock Salt under Different Healing Conditions. **Materials.** 6:3438 – 3450.
- Fuenkajorn, K. (2007). INTRINSIC VARIABILITY OF THE MECHANICAL PROPERTIES OF MAHA SARAKHAM SALT. **Suranaree Journal of Science and Tecnology.** 15(1): 33-48.
- Fuenkajorn, K. and Kenkhunthod, N. (2010). Influence of loading rate on deformability and compressive strength of three Thai sandstones. **Geotechnical and Geological Engineering.** 28: 707–715.
- Fuenkajorn, K. and Phueakphum, D. (2011). Laboratory assessment of healing of fracture in rock salt. **Bulletin of Engineering Geology and the Environment,** 70: 665-672.
- Habib, P. and Berest, P. (1993). Rock mechanics for underground nuclear waste disposal in France: Developments and case studies. **Comprehensive Rock Engineering, Geothermal Energy and Radioactive Waste Disposal.** Great Britain, Pergamon. 5: 547-563.

- Jiang, D., Li, L., Chen, J., Ren, S., and Yang, C (2013). Self-recovery ability of stress-damaged salt rock experiment. **Journal of Coal Science & Engineering (China)**. pp. 63–68.
- Katz, D.L., Lady, E.R. (1976). Compressed air storage for electric power generation. **Department of Energy Pacific Northwest**. Richland, Washington.
- Miao, S., Wang, M.L., Schreyer, H.L. (1995). Constitutive models for healing of materials with application to compaction of crushed rock salt. **Journal of Engineering Mechanics**. 10 (121): 1122–1129
- Munson, D.E., Chan, K.S., Fossum AF (1999). Fracture and healing of rock salt related to salt caverns. **Solution Mining Research Institute**. Encinitas, California.
- Phueakphum, D. (2003). **Compressed-air energy storage in rock salt of the Mahasarakham formation**. M.S. Thesis. Suranaree University of Technology, Thailand. pp. 153.
- Renard, F. (1999). Pressure solution and crack healing and sealing. **Institute of Geology and Department of Physics**. University of Oslo, Norway.
- Zeigler, T.W.** (1976). Determination of rock mass permeability (Technical Report S-76-2). **U.S. Army Engineer Waterways Experiment Station**. Vicksburg, Mississippi.

BIOGRAPHY

Mr. Prueangprach Charoenpiew was born on May 5, 1989 in Mahasarakham province, Thailand. He received his Bachelor's Degree in Engineering (Geotechnology) from Suranaree University of Technology in 2012. For his post-graduate, he continued to study with a Master's degree in the Geological Engineering Program, Institute of Engineering, Suranaree university of Technology. During graduation, 2013-2015, he was a part time worker in position of research assistant at the Geomechanics Research Unit, Institute of Engineering, Suranaree University of Technology.

